© 2014. Published by The Company of Biologists Ltd | Development (2014) 141, 538-547 doi:10.1242/dev.099481

RESEARCH ARTICLE

STEM CELLS AND REGENERATION

Prox1 ablation in hepatic progenitors causes defective hepatocyte specification and increases biliary cell commitment

Asha Seth[1,*], Jianming Ye[1,*], Nanjia Yu[1], Fanny Guez[1], David C. Bedford[2], Geoffrey A. Neale[3], Sabine Cordi[4], Paul K. Brindle[2], Frederic P. Lemaigre[4], Klaus H. Kaestner[5] and Beatriz Sosa-Pineda[1,‡]

ABSTRACT

The liver has multiple functions that preserve homeostasis. Liver diseases are debilitating, costly and often result in death. Elucidating the developmental mechanisms that establish the liver's architecture or generate the cellular diversity of this organ should help advance the prevention, diagnosis and treatment of hepatic diseases. We previously reported that migration of early hepatic precursors away from the gut epithelium requires the activity of the homeobox gene *Prox1*. Here, we show that Prox1 is a novel regulator of cell differentiation and morphogenesis during hepatogenesis. *Prox1* ablation in bipotent hepatoblasts dramatically reduced the expression of multiple hepatocyte genes and led to very defective hepatocyte morphogenesis. As a result, abnormal epithelial structures expressing hepatocyte and cholangiocyte markers or resembling ectopic bile ducts developed in the *Prox1*-deficient liver parenchyma. By contrast, excessive commitment of hepatoblasts into cholangiocytes, premature intrahepatic bile duct morphogenesis, and biliary hyperplasia occurred in periportal areas of *Prox1*-deficient livers. Together, these abnormalities indicate that Prox1 activity is necessary to correctly allocate cell fates in liver precursors. These results increase our understanding of differentiation anomalies in pathological conditions and will contribute to improving stem cell protocols in which differentiation is directed towards hepatocytes and cholangiocytes.

KEY WORDS: Prox1, Liver, Hepatic precursors, TGFβ, Mouse

INTRODUCTION

Mouse liver morphogenesis initiates at approximately embryonic day (E) 8.5, with the transition of a region of the hepatic endoderm into columnar epithelium, the onset of expression of *Hnf4a*, albumin and alpha-fetoprotein (*Afp*), and the subsequent thickening and bulging of the hepatic epithelium. By E10.0, the basal membrane surrounding the hepatic diverticulum begins to disappear; the level of E-cadherin (Cadherin 1 – Mouse Genome Informatics) expression is downregulated; and the hepatic precursors (or hepatoblasts) start to delaminate and invade the surrounding stromal tissue (Si-Tayeb et al., 2010).

Hepatoblasts are bipotent precursors that develop into either hepatocytes (the main epithelial cells in the liver) or cholangiocytes (the epithelial cells lining the intrahepatic biliary ducts). The formation of hepatocytes and cholangiocytes is temporally and spatially separated, which suggests that localized inducers or repressing mechanisms operate to direct either fate (Zaret, 2002). A network of liver-enriched transcription factors comprising six core regulators [Hnf1α, Hnf1β, FoxA2, Hnf4α, Hnf6 (Onecut1 – Mouse Genome Informatics) and Nr5a2 (also known as Lrh-1)] guides the differentiation of parenchymal hepatoblasts into hepatocytes (Kyrmizi et al., 2006). This transcriptional network is very dynamic; it involves increasing cross-regulatory interactions necessary to establish hepatocyte maturation (Kyrmizi et al., 2006).

Bile duct formation begins at ~E14.5 in a transient periportal structure called the ductal plate. This process involves several signaling pathways, among which TGFβ/activin signaling affects cholangiocyte and hepatocyte differentiation (Clotman et al., 2005; Lemaigre, 2009). In the ductal plate, hepatoblasts activate the expression of the transcription factor Sox9 and inactivate that of Hnf4α. Asymmetric primitive ductal structures (PDSs) then emerge from the ductal plate; these PDSs comprise a periportal $Sox9^+$ cell layer covered with a basal membrane rich in laminin and nidogen proteins (Shiojiri and Sugiyama, 2004) and a parenchymal $Hnf4\alpha^+/Sox9^-$ cell layer lacking a basal membrane. PDSs gradually remodel to form the intrahepatic bile ducts by acquiring radial symmetry, establishing apicobasal polarity and forming a lumen. The activity of the transcription factors Sox9, Hnf6 and Hnf1β is necessary for proper biliary development, and Notch signaling is important for both bile duct remodeling and cholangiocyte differentiation (Lemaigre, 2009).

The homeobox gene *Prox1* is a crucial regulator of cell differentiation and morphogenesis in various tissues (Sosa-Pineda et al., 2000; Lavado et al., 2010; Wigle and Oliver, 1999; Westmoreland et al., 2012), and it is one of the earliest markers of vertebrate hepatic development (Burke and Oliver, 2002). We previously demonstrated that the loss of Prox1 activity disrupts the delamination of hepatoblasts from the hepatic diverticulum, which hampers their migration and causes an early arrest of liver development (Sosa-Pineda et al., 2000). *Prox1* is also expressed in the hepatocytes of the adult liver, with recent evidence supporting the theory that in these cells Prox1 negatively regulates the activity of ERRα (Esrra – Mouse Genome Informatics) (Charest-Marcotte et al., 2010), Hnf4α (Song et al., 2006) and Nr5a2 (Qin et al., 2004), three nuclear receptors controlling various hepatic metabolic functions. More recently, we determined that Prox1 function controls ductal cell development in a similar endoderm-derived organ, the pancreas (Westmoreland et al., 2012).

In this study, we explored the hypothesis that *Prox1* activity is required for cell differentiation, morphogenesis or both in the fetal liver. By conditionally deleting the gene from hepatoblasts developed beyond the stage when they are released from the liver diverticulum, we found a novel, distinct role of Prox1 in the allocation of epithelial cell types during hepatogenesis.

[1]Department of Genetics, St Jude Children's Research Hospital, Memphis, TN 38105, USA. [2]Department of Biochemistry, St Jude Children's Research Hospital, Memphis, TN 38105, USA. [3]Hartwell Center for Bioinformatics and Biotechnology, St Jude Children's Research Hospital, Memphis, TN 38105, USA. [4]de Duve Institute, Universite Catholique de Louivan, 1200 Brussels, Belgium. [5]Department of Genetics, University of Pennsylvania, Philadelphia, PA 19104, USA.
*These authors contributed equally to this work

‡Author for correspondence (beatriz.sosa-pineda@stjude.org)

Received 26 May 2013; Accepted 14 November 2013

Development (2014) doi:10.1242/dev.099481

RESULTS

Prox1 is expressed in epithelial liver cells throughout life

We previously reported Prox1 expression in the hepatic primordium and the emerging liver bud in E9.0-E10.5 wild-type embryos (Sosa-Pineda et al., 2000). Here, we examined the distribution of Prox1 proteins in fetal and adult mouse livers using immunostaining methods. Prox1 was expressed in all hepatoblasts (Ecadherin$^+$ cells) in E10.0-E12.5 livers (Fig. 1A,B). Prox1 was also detected in all hepatocytes in E15.5-E18.5 livers (Hnf4α$^+$ cells; Fig. 1C-E; data not shown) and cholangiocytes (Sox9$^+$ cells) forming ductal plates (Fig. 1D), PDSs (Fig. 1D,E) or bile ducts (Fig. 1E) in E15.5-E18.5 livers. In adult livers, Prox1 expression was high in hepatocytes (Fig. 1F, arrowheads) and comparatively lower in intrahepatic bile ducts (Fig. 1F, arrows). This last finding is in contrast with a report showing Prox1 expression in hepatocytes, and absence of this protein in cholangiocytes, in the liver of adult rats (Dudas et al., 2004). It is probable that variability in the sensitivity of the immunodetection methods used in each study accounted for the discrepant results.

The persistent expression of Prox1 in hepatic cells suggested that, in addition to hepatoblast delamination (Sosa-Pineda et al., 2000), other aspects of liver development require Prox1 activity. To investigate this possibility, we generated *Prox1*$^{loxP/loxP}$*;Foxa3Cre* mice (hereafter designated as *Prox1*$^{\Delta LIV}$) carrying *Prox1*-specific ablation in foregut endoderm-derived tissues.

Prox1$^{\Delta LIV}$ mice have defective liver morphology and die at birth

The onset of Prox1 deletion was examined in *Prox1*$^{\Delta LIV}$ livers using a combination of immunostaining, lineage tracing and qRT-PCR methods. These analyses showed similar distribution and abundance of Prox1$^+$ cells between control and *Prox1*$^{\Delta LIV}$ livers at E10.5 (supplementary material Fig. S1A,B). By contrast, Prox1$^+$ cells were numerous in E12.5-E18.5 control livers (supplementary material Fig. S1C and Fig. S2A,C,E) and scarce or absent in livers of *Prox1*$^{\Delta LIV}$ littermates (supplementary material Fig. S1D and Fig. S2B,D,F, arrows). The qRT-PCR results also showed that *Prox1* transcripts began to diminish after E11.5 and were reduced by >90% at E13.5 in *Prox1*$^{\Delta LIV}$ livers (supplementary material Fig. S1E). Therefore, *Prox1* was deleted in hepatoblasts of *Prox1*$^{\Delta LIV}$ livers after delamination occurred.

Unlike control livers (supplementary material Fig. S2A,C,E), E12.5-E18.5 *Prox1*-deficient livers contained numerous cellular aggregates covered with a basal membrane rich in laminin (not shown) and nidogen (supplementary material Fig. S2B,D,F). These abnormal structures were first observed at ~E12.5 close to the hilum, but later (E15.5-E18.5) they were also detected in more peripheral areas of the mutant liver (supplementary material Fig. S2). Interestingly, although some Prox1-expressing cells remained in *Prox1*$^{\Delta LIV}$ livers, they never localized within the previous epithelial structures (supplementary material Fig. S2F). Thus, the lack of *Prox1* activity promotes the formation of a basal membrane in hepatoblasts.

All *Prox1*$^{\Delta LIV}$ mice died at birth, and their livers were considerably smaller than those of control littermates (Fig. 2A,B). Compared with control livers, E18.5-postnatal day (P) 0 *Prox1*$^{\Delta LIV}$ livers displayed very unusual tissue architecture (Fig. 2C,D), prominent deposits of fibronectin in the parenchyma (Fig. 2E,F), and excessive mesenchyme (Fig. 2G,H). Microarray analyses also revealed increased expression of transcripts encoding extracellular matrix/basal membrane proteins, cell adhesion proteins and metalloproteases in *Prox1*-deficient livers at E14.5 (supplementary material Table S2). Thus, the multiple alterations identified in *Prox1*$^{\Delta LIV}$ livers indicate that hepatic morphogenesis requires constant Prox1 activity.

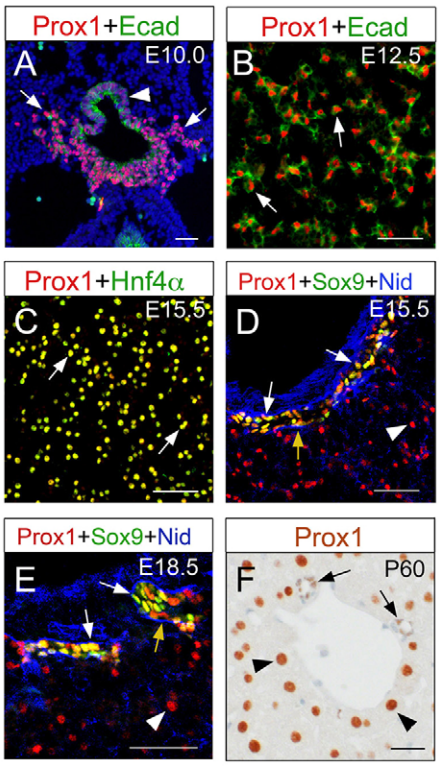

Fig. 1. Prox1 is expressed in epithelial cells of the fetal and adult mouse liver. (A) Prox1 is highly expressed in hepatoblasts (arrows) of E10.0 livers. Prox1 levels are lower in the adjacent gut epithelium (arrowhead). (B) Prox1 is broadly expressed in epithelial cords [Ecadherin$^+$ (Ecad), arrows] of E12.5 livers. (C) Prox1 co-expresses with Hnf4α in all hepatocytes (arrows) of E15.5 livers. (D) Prox1 also co-expresses with Sox9 in primitive ductal structures (PDSs; arrows) of E15.5 livers. Yellow arrow points to the nidogen-rich (Nid) basal membrane, and an arrowhead points to a Prox1$^+$ hepatocyte. (E) Cells co-expressing Prox1 and Sox9 localize to PDSs (arrow on the left) and developing bile ducts (arrow on the right; yellow arrow points to the Nid$^+$ basal membrane) of E18.5 livers (arrowhead points to a Prox1$^+$ hepatocyte). (F) Hepatocytes express high Prox1 (arrowheads), and bile ducts express low Prox1 (arrows) in adult livers. Cell nuclei were stained with DAPI (A, blue) or hematoxylin (F). Scale bars: 25 µm (F); 50 µm (A-E).

Prox1 deletion in hepatoblasts decreases hepatocyte formation and increases cholangiocyte cell numbers

Abnormal liver morphology combined with defective hepatocyte differentiation could explain the perinatal lethality of *Prox1*$^{\Delta LIV}$ mice. Therefore, the expression of genes encoding key regulators of hepatocyte development, including the core components of the hepatocyte regulatory network (Kyrmizi et al., 2006), was examined in fetal livers following *Prox1* ablation (E12.5). The qRT-PCR data showed relatively normal expression of *Hnf1a*, *Foxa2*, *Nr5a2*, *Cebpa*, *Esrra*, *Gata6*, *Hhex* and *Tbx3* in *Prox1*$^{\Delta LIV}$ livers (Fig. 3A). By contrast, *Prox1* ablation decreased the expression of *Hnf4a* and increased the expression of *Hnf6*, *Hnf1b* and *Nr2f2* (also known as *COUP-TFII*) (Fig. 3A). Combined qRT-PCR and microarray results revealed deficient expression of numerous hepatocyte metabolic transcripts in *Prox1*-deficient livers at E12.5-E15.5 (Fig. 3C,D; supplementary material Table S3A). These data argue that Prox1 activity is necessary for proper hepatocyte differentiation.

Development (2014) doi:10.1242/dev.099481

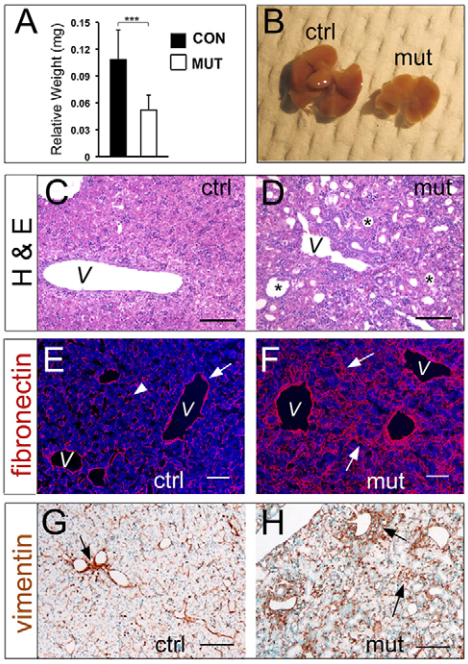

Fig. 2. *Prox1*-depleted livers have severely disrupted architecture. (A,B) E18.5 *Prox1*$^{\Delta LIV}$ (mut) livers have both significantly reduced weight (A) and smaller size (B) in comparison with E18.5 control (ctrl) livers. (C,D) Hematoxylin and Eosin staining reveals that the tissue architecture of E18.5 *Prox1*$^{\Delta LIV}$ livers (D) is severely disrupted compared with control livers (C). Asterisks indicate cysts or ducat structures in the mutant liver parenchyma. (E-H) Compared with control livers (E,G), E18.5-P0 *Prox1*$^{\Delta LIV}$ livers display extensive fibronectin deposition (F, arrows) and abundance of mesenchymal cells (vimentin^{+}; H, arrows) in the parenchyma. Arrow in G indicates the periportal mesenchyme (vimentin^{+}); arrowhead in E indicates laminin expression in sinusoids. *V*, portal vein. (E-H) Cell nuclei were stained with DAPI (E,F) or Methyl Green (G,H). $P<0.001$; $n=3$-4. Scale bars: 100 µm.

In contrast to its effects on *Hnf4a* expression, *Prox1* deletion significantly increased the expression of the biliary transcripts *Sox9*, *Lamb1* and *Krt19* in E12.5-E15.5 *Prox1*$^{\Delta LIV}$ livers (Fig. 3B; supplementary material Table S3B). Likewise, *Cldn7* transcripts, encoding a tight junction protein, which is identified here as a novel biliary marker, were increased in *Prox1*-depleted livers compared with control livers (Fig. 3B; supplementary material Table S2B).

Opposite effects in hepatocyte versus cholangiocyte gene expression resulting from *Prox1* deletion suggested that cholangiocyte formation increases at the expense of hepatocyte differentiation in *Prox1*$^{\Delta LIV}$ livers. To verify this hypothesis, the distribution of hepatocytes (Hnf4α^{+}) and cholangiocytes (Sox9^{+}) was compared between control and *Prox1*$^{\Delta LIV}$ livers using immunostaining methods. Hnf4α^{+} cells were abundant throughout the parenchyma, formed epithelial cords lacking a basal membrane, and were absent around the portal veins (Fig. 4A,C,E) in E12.5-E18.5 control livers. By contrast, Sox9^{+} cells were noticeably less numerous than Hnf4α^{+} cells and were restricted to periportal areas (Fig. 4G,I,K) in E12.5-E18.5 control livers.

Unlike control livers, *Prox1*$^{\Delta LIV}$ livers showed a gradual decrease in the abundance of Hnf4α^{+} cells (Fig. 4B,D,F). This defect was more pronounced in the parenchymal structures displaying a basal membrane (Fig. 4D,F, arrowheads). We also observed fewer cells expressing the hepatocyte marker C/EBPα in the parenchyma of *Prox1*-deficient livers (supplementary material Fig. S3A-D). By contrast, Sox9^{+} cells were more numerous in *Prox1*$^{\Delta LIV}$ livers than in controls at E12.5-E18.5 (Fig. 4H,J,L, arrows). Furthermore, unlike control livers, *Prox1*-deficient livers had Sox9^{+} cells not only around the portal veins but also in the parenchyma (Fig. 4J,L, arrowheads). These results strongly suggest that the lack of Prox1 activity diverts the specification of parenchymal hepatoblasts from hepatocytes to cholangiocytes.

Bile ducts form prematurely in *Prox1*$^{\Delta LIV}$ livers

Sox9^{+} cells were increased in *Prox1*$^{\Delta LIV}$ livers; therefore, we immunostained the mutant tissues to investigate whether intrahepatic bile duct formation was affected. Cholangiocytes expressing Sox9 were initially detected at ~E12.5 in periportal areas close to the hilum (Fig. 4G) and later (E15.5-E18.5) around portal veins located in more peripheral areas in control livers (Fig. 4I,K). The few Sox9^{+} cells in periportal areas of E12.5 control livers were scattered (Fig. 4G; Fig. 5A) or started to form ductal plates (data not shown). By E15.5, most cholangiocytes formed ductal plates (Fig. 4I; Fig. 5B, arrow) or asymmetric ductal structures displaying a basal membrane on the periportal side (Fig. 5C, arrow) but not bile ducts in control livers. At this stage, cholangiocytes expressed Sox9 (Fig. 4I), high levels of Hnf1β (Fig. 5B), and claudin 7 (Fig. 5C) but not Hnf4α (Fig. 5B,C). At E18.5, we observed numerous incipient bile ducts around the portal veins of control livers expressing Sox9 (Fig. 4K; Fig. 5G,H) and claudin 7 (Fig. 5I) but not Hnf4α (Fig. 5G,I). Bile ducts of E18.5 control livers displayed apical distribution of osteopontin proteins (Fig. 5H), were surrounded by a nidogen-expressing basolateral membrane (Fig. 5G,I), and had small but well-defined lumens (Fig. 5G-I).

Unlike control livers, all Sox9^{+} cells in periportal areas of E12.5 *Prox1*$^{\Delta LIV}$ livers formed large epithelial aggregates covered with a nidogen-rich basal lamina (Fig. 4H; Fig. 5D). As early as E15.5, we observed well-developed intrahepatic bile ducts (Fig. 5E,F, arrows) around the portal veins in *Prox1*$^{\Delta LIV}$ livers. The ducts of *Prox1*-deficient livers expressed numerous biliary markers, including Sox9 (Fig. 4J), high Hnf1β (Fig. 5E), and claudin 7 (Fig. 5F) but not Hnf4α (Fig. 5E,F), had visible lumens (Fig. 5E,F) and expressed apical osteopontin (Fig. 5K).

In addition to forming prematurely, the intrahepatic bile ducts of *Prox1*$^{\Delta LIV}$ livers were larger than those of control livers. This defect was first noticed at ~E15.5 (Fig. 4I,J) and was obvious at E18.5 [compare the size of the bile ducts (arrows) between control (Fig. 5G-I) and *Prox1*$^{\Delta LIV}$ (Fig. 5J-L) livers]. Quantitative proliferation analyses determined that the mitotic ratios of periportal Sox9^{+} cells did not differ between control and *Prox1*$^{\Delta LIV}$ fetal livers (data not shown). Thus, increased cholangiocyte commitment of precursors, but not enhanced cell proliferation, probably caused biliary hyperplasia in *Prox1*$^{\Delta LIV}$ livers.

Prox1 ablation promotes the formation of ectopic biliary structures in the liver parenchyma

The epithelial aggregates in the parenchyma of *Prox1*$^{\Delta LIV}$ livers that were surrounded with a basal membrane (supplementary material Fig. S3C,D,G,H,K,L, arrowheads), had abundant cells expressing high levels of Hnf6 (supplementary material Fig. S3G,H) and Hnf1β (supplementary material Fig. S3K,L) and only a few cells expressing C/EBPα (supplementary material Fig. S3C,D). Some of these parenchymal structures resembled bona fide bile ducts, because they expressed Sox9 (Fig. 4J,L), osteopontin and claudin 7 (Fig. 6G-I), lacked Hnf4a expression (Fig. 6F), displayed apicobasal polarity (Fig. 6H,I), and had prominent lumens (Fig. 6F, asterisks; supplementary material Fig. S3H). Most of these ductal structures were located in the hilar region (Fig. 4L) or in proximity to veins

Development (2014) doi:10.1242/dev.099481

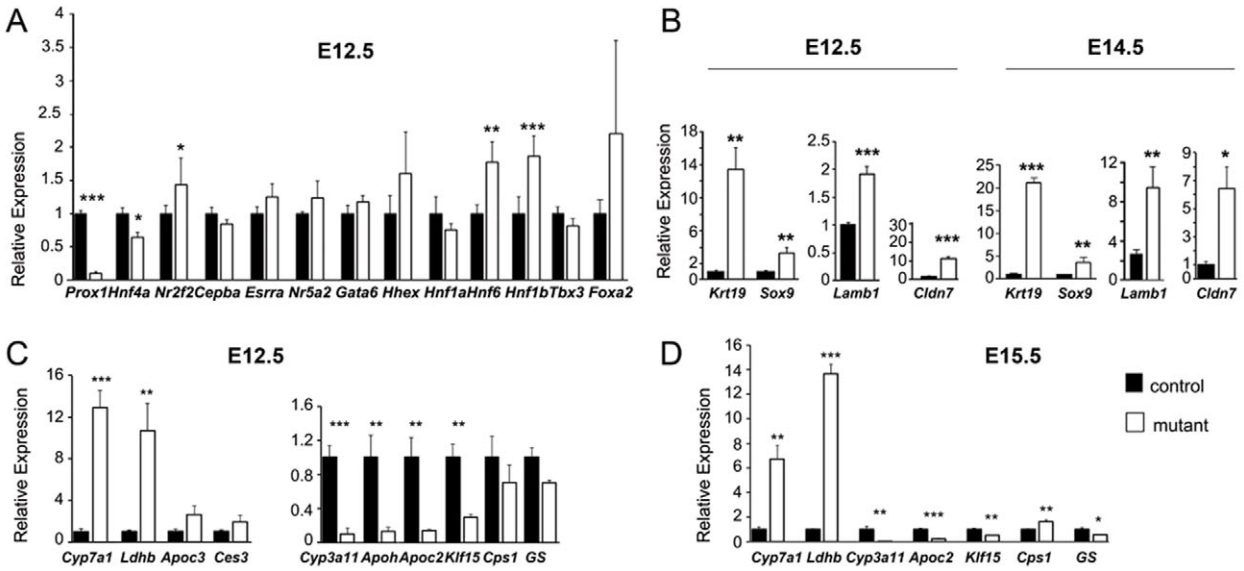

Fig. 3. *Prox1* ablation in hepatic precursors increases biliary gene expression and affects hepatocyte metabolic gene expression. (A) qRT-PCR data show reduced expression of *Hnf4a* and increased expression of *Hnf6*, *Hnf1b* and *Nr2f2* in *Prox1*$^{\Delta LIV}$ livers dissected at E12.5. (B-D) qRT-PCR data also show increased expression of the biliary markers *Krt19*, *Sox9*, *Lamb1* and *Cldn7* (B) and defective expression of various hepatocyte metabolic transcripts (C,D) in *Prox1*$^{\Delta LIV}$ livers dissected at E12.5-E15.5 compared with control livers (*n*=3-4 liver specimens; **P*<0.05, ***P*<0.01, ****P*<0.001).

(Fig. 4J) in *Prox1*$^{\Delta LIV}$ livers. Therefore, *Prox1* ablation in hepatic progenitors promotes the formation of ectopic bile ducts in the liver parenchyma.

A different class of epithelial structure was also identified in the parenchyma of E15.5-E18.5 *Prox1*$^{\Delta LIV}$ livers. These were aggregates covered with a basal membrane, harboring cells that expressed the hepatocyte markers Hnf4α and C/EBPα (Fig. 6B,C) but lacking Prox1 expression (supplementary material Fig. S2D,F). In addition to hepatocytes (i.e. Hnf4α^{+}/Sox9^{-} cells) and cholangiocytes (i.e. Sox9^{+}/Hnf4α^{-} cells), 'hybrid' cells (i.e. Sox9^{+}/Hnf4α^{+} cells) were identified within the previous parenchymal aggregates of *Prox1*$^{\Delta LIV}$ livers (Fig. 6D,E). These data argue that not all parenchymal hepatoblasts fully commit to biliary cells in *Prox1*$^{\Delta LIV}$ livers.

TGFβ signaling gradually increases in fetal liver lacking *Prox1*

TGFβ signaling promotes biliary differentiation (Lemaigre, 2009), and here we extended this notion by showing that TGFβ and activin A stimulate *Sox9*, *Krt19* and *Lamb1* expression in explants from E12.5 wild-type livers (Fig. 7A). Several results also indicated that TGFβ activity increases in *Prox1*$^{\Delta LIV}$ livers after E12.5. First, microarray analyses showed an increment of the TGFβ targets *Sox9*, *Krt19*, *Lamb1*, *Tgfbi* (Carey and Chang, 1998) and *Gli2* (Dennler et al., 2009) in E14.5 *Prox1*$^{\Delta LIV}$ livers (supplementary material Table S4). Second, western blot analysis showed increased expression of phospho-Smad2/3 in E13.5-E14.5 *Prox1*$^{\Delta LIV}$ livers (Fig. 7B). Third, microarray and qRT-PCR analyses showed increased expression of transcripts encoding ligands and receptors of TGFβ signaling in *Prox1*$^{\Delta LIV}$ livers at E14.5-E15.5 (supplementary material Table S4; Fig. 7C) but not at E12.5 (supplementary material Fig. S4A). By contrast, no evidence was found that expression of ligands or receptors of Notch signaling, another potent inducer of biliary development (Tanimizu and Miyajima, 2004; Zong et al., 2009; Tchorz et al., 2009; Lozier et al., 2008), increase in *Prox1*$^{\Delta LIV}$ livers (supplementary material Fig. S4B; data not shown). Furthermore, although *Hes1* transcripts were slightly more abundant in *Prox1*$^{\Delta LIV}$ livers than in control livers at E12.5 (supplementary material Fig. S4B), this change was very small (1.4-fold) and was probably a consequence, not a cause, of enhanced cholangiocyte commitment.

The results of microarray, qRT-PCR and *in situ* hybridization approaches uncovered deficient expression of transcripts encoding the activin inhibitor follistatin (Fst) (Nakamura et al., 1990) and the TGFβ inhibitor alpha-2-HS-glycoprotein (Ahsg) (Szweras et al., 2002) in E12.5-E14.5 *Prox1*$^{\Delta LIV}$ livers (Fig. 7D; supplementary material Fig. S5B and Table S4). These results suggest that in *Prox1*$^{\Delta LIV}$ livers, an excessive production of TGFβ ligands combined with deficient expression of inhibitors of this pathway contributed to increasing cholangiocyte commitment in periportal areas and helped to confer biliary cell fate to parenchymal hepatoblasts.

Prox1 ablation in committed hepatocytes does not shift the fate of these cells towards cholangiocytes

We previously showed that hepatoblast delamination is defective in the liver of *Prox1*-nullizygous embryos (Sosa-Pineda et al., 2000). This alteration prevented the migration of hepatoblasts towards the liver periphery and retained those cells close to the hilum. We investigated whether biliary development was also affected in the liver of mouse embryos with germline deletion of *Prox1* (*Prox1*$^{GFP/GFP}$) (Srinivasan et al., 2010). All hepatoblasts (GFP^{+} cells) in the E11.5 *Prox1*$^{GFP/GFP}$ liver (Fig. 8B-D), but not in the control liver (Fig. 8A), formed a structure covered by a nidogen-rich basal membrane, which remained contiguous to the gut epithelium (Fig. 8B,D). At this stage, cells within the mutant hepatic epithelium expressed Hnf4α (Fig. 8C) and negligibly expressed Sox9 (data not shown) or the gall bladder marker Sox17 (Fig. 8D) (Spence et al., 2009; Uemura et al., 2010).

By E14.5, *Prox1*$^{GFP/GFP}$ livers were largely devoid of epithelial cells except in the hilar region, where a GFP^{+} epithelium covered with a basal membrane and displaying prominent lumens remained adjoined to the gall bladder (Fig. 8E). At this stage, numerous cells

Development (2014) doi:10.1242/dev.099481

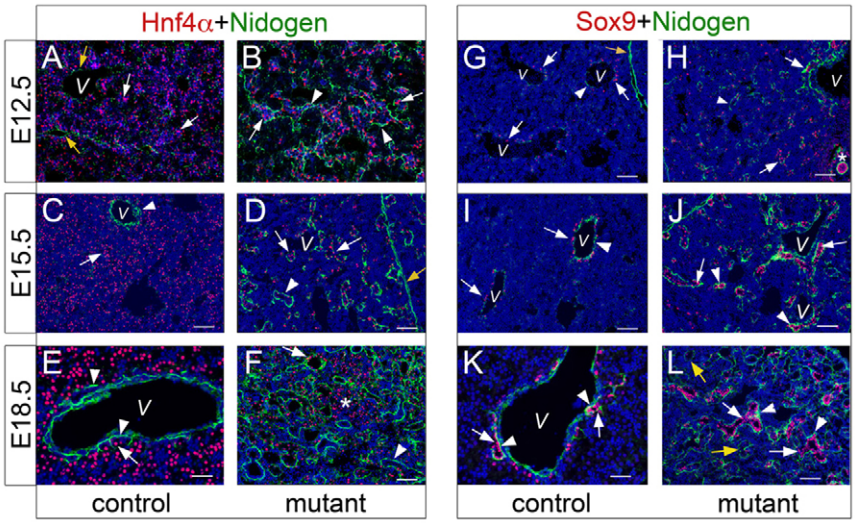

Fig. 4. *Prox1*-depleted livers have defective expression of Sox9 and Hnf4α and abnormal parenchymal epithelial structures. (A,C,E) Cells expressing Hnf4α (arrows) are abundant throughout the parenchyma and are absent in periportal areas where bile ducts should develop (yellow arrows in A and arrowheads in C,E) in E12.5-E18.5 control livers. (B,D,F) The abundance of Hnf4α$^+$ cells decline between E12.5 and E18.5 in the nidogen-rich epithelial aggregates (arrowheads) of *Prox1*$^{\Delta LIV}$ livers (asterisk in F indicates a cluster of Hnf4α$^+$ cells lacking a basal membrane). Yellow arrow indicates nidogen expression at the periphery of the lobe. (G,I,K) A small population of cells expressing Sox9 (arrows) and restricted to periportal areas is observed in E12.5-E18.5 control livers [arrowheads indicate nidogen expression in the vein endothelium (G,I) or around the incipient bile ducts (K); yellow arrow in G indicates nidogen expression at the edge of the liver lobes]. (H,J,L) Sox9$^+$ cells (arrows) are increasingly abundant and form aggregates surrounded by a nidogen-rich basal membrane (arrowheads) around the portal veins (H,J) and in the parenchyma (H,J,L) in E12.5-E18.5 *Prox1*$^{\Delta LIV}$ livers (yellow arrows in L indicate epithelial aggregates devoid of Sox9 expression). *V*, portal vein branches. Cell nuclei were stained with DAPI. Scale bars: 50 µm (E,K); 100 µm (A-D,F-J,L).

in the *Prox1*-nullizygous hepatic epithelium were Sox9$^+$/Hnf4α$^-$ (Fig. 8F) and expressed the biliary marker *Dolichos biflorus* agglutinin (data not shown). By contrast, the vast majority of Sox9$^+$ cells in the E14.5 wild-type liver formed ductal plates but not ducts (Fig. 8F, inset). These results indicate that the entire *Prox1*-nullizygous hepatic epithelium evolved into a biliary structure reminiscent of the hyperplastic bile ducts of the *Prox1*$^{\Delta LIV}$ liver.

We also generated *Prox1*$^{f/f}$*;AlbCre* mice to investigate whether the formation of hepatocytes and cholangiocytes is affected when *Prox1* is deleted in newly committed hepatic cells (supplementary material Fig. S6A,B). The results of qRT-PCR showed negligible changes in *Prox1* expression at E13.5 and significant reduction of *Prox1* expression at E19.5 (supplementary material Fig. S6E) in *Prox1*$^{f/f}$*;AlbCre* livers. Immunostaining results also corroborated that very few cells expressed Prox1 in E18.5 *Prox1*$^{f/f}$*;AlbCre* livers (Fig. 8G,J). However, in contrast to our findings in *Prox1*$^{\Delta LIV}$ livers, deleting *Prox1* in committed hepatic cells (i.e. after E13.5) did not affect the expression of Hnf4α (Fig. 8G,J), nidogen (Fig. 8H,K) or Sox9 (Fig. 8I,L) in the liver. Thus, only the allocation of hepatocytes and cholangiocytes is affected when *Prox1* is ablated in hepatoblasts.

DISCUSSION

Early hepatic morphogenesis and cell specification are tightly coupled processes requiring Prox1 activity

Prox1 is an essential component of the regulatory network controlling early hepatic morphogenesis together with Hhex, Tbx3, Hnf6, OC-2 (Onecut2 – Mouse Genome Informatics) and Gata6 (Lemaigre, 2009). Lüdke et al. (Lüdtke et al., 2009) postulated that in this network *Tbx3* acts upstream of *Prox1* because, similar to our report in *Prox1*-null mice (Sosa-Pineda et al., 2000), the hepatic precursors of *Tbx3*-null embryos had reduced proliferation, and these cells did not delaminate from the gut endoderm (Lüdtke et al., 2009; Suzuki et al., 2008). Also, the loss of *Tbx3* function did not affect the onset of *Prox1* expression in the hepatic endoderm but failed to maintain its expression in the liver bud after E9.5 (Lüdtke et al., 2009). Our finding that *Prox1* deletion in hepatoblasts did not affect the expression of *Tbx3* also supports the notion that this gene is located upstream of *Prox1* in the regulatory network controlling early liver morphogenesis.

In addition to a blockage in hepatoblast delamination, increased expression of genes controlling biliary development (i.e. *Hnf6* and *Hnf1b*) and reduced expression of genes required for hepatocyte development (i.e. *Hnf4a* and *Cebpa*) was uncovered in *Tbx3*-null livers (Lüdtke et al., 2009). Therefore, the inability of *Tbx3*-null hepatoblasts to delaminate from the gut endoderm was suggested to be a consequence of their failure to initiate hepatocyte differentiation. Likewise, here we showed that *Prox1*-null hepatoblasts failed to delaminate but instead developed into a ductal structure in which cholangiocytes (Sox9$^+$) were more abundant than hepatocytes (Hnf4α$^+$). Moreover, when Prox1 was deleted in hepatoblasts post-delamination the cells rapidly deposited basal membrane proteins and formed atypical aggregates in the parenchyma, and these alterations were accompanied by increased expression of Hnf6 and Hnf1β and reduced expression of Hnf4α and C/EBPα. Therefore, our study revealed that Prox1 is a novel key regulator of processes coupling hepatic cell specification and hepatic morphogenesis.

Is cholangiocyte specification the default fate of hepatoblasts?

Prox1-depleted hepatoblasts formed aggregates, rather than loose epithelial cords, that rapidly became surrounded with a prominent basal membrane. Currently, we do not know if the unusual deposition of a basal membrane around those mutant hepatoblasts was a direct effect or was secondary to the loss of Prox1 activity. However, signals downstream of TGFβ may have contributed to this

Development (2014) doi:10.1242/dev.099481

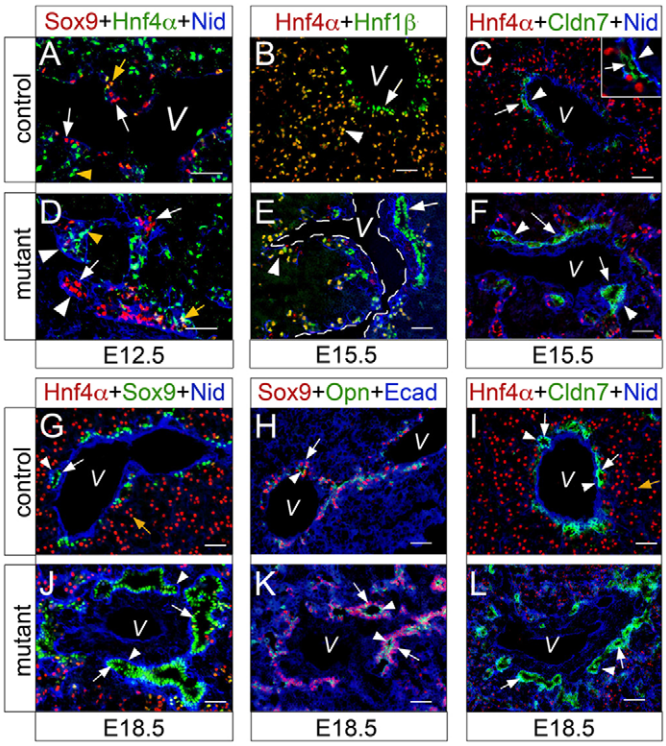

Fig. 5. Intrahepatic bile ducts form prematurely and have defective morphology in the absence of *Prox1*. (A-I) Cholangiocytes expressing Sox9 (arrows) are not very numerous around the portal vein branches (*V*) in the hilar region of E12.5 control livers (A; yellow arrow indicates a Sox9$^+$/Hnf4α$^+$ periportal cell, and yellow arrowhead indicates an Hnf4α$^+$/Sox9$^-$ parenchymal cell). In control livers, cholangiocytes form ductal plates (arrows in B,C) or PDS displaying a basal membrane on the periportal side (arrowhead in C) at E15.5 and start forming bile ducts (arrows in G-I at ~E18.5). In addition to Sox9 (A,G,H), cholangiocyes express Hnf1β (arrow in B), claudin 7 (arrows in C,I), osteopontin (arrowhead in H), but not Hnf4α (C,G,I), in E12.5-E18.5 control livers. (D) Large epithelial aggregates surrounded by a prominent nidogen-rich basal membrane (arrowheads) and containing abundant Sox9$^+$ cells (arrows), Hnf4α$^+$ cells (yellow arrowhead), and a few Sox9$^+$/Hnf4α$^+$ cells (yellow arrow) are seen around portal veins in the hilar region of E12.5 *Prox1*$^{\Delta LIV}$ liver. (E,F) Cholangiocytes form ductal structures (arrows) surrounded by a nidogen-rich basolateral membrane (arrowheads, blue staining), around the portal vein branches in E15.5 *Prox1*$^{\Delta LIV}$ livers. (J-L) E18.5 *Prox1*$^{\Delta LIV}$ livers have abnormally large intrahepatic bile ducts (arrows) surrounding the portal vein branches (arrowheads indicate the basolateral membrane). (E) Triple immunofluorescence staining for Hnf4α (red), Hnf1β (green) and nidogen (blue). Scale bars: 50 μm (A-K); 100 μm (L).

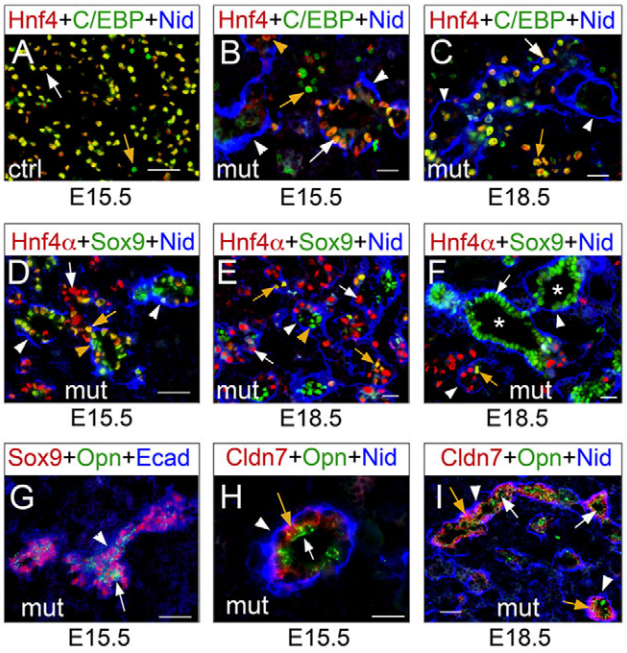

Fig. 6. Ectopic bile ducts form in the liver parenchyma in the absence of *Prox1*. (A) Numerous hepatocytes (white arrow) expressing Hnf4α and C/EBPα and lacking a basal membrane colonize the E15.5 liver parenchyma [C/EBPα$^+$/Hnf4α$^-$ cells (yellow arrow) are not hepatocytes]. (B,C) Fewer Hnf4α$^+$/C/EBPα$^+$ cells (white arrows) are observed within the parenchymal aggregates of E15.5 (B) and E18.5 (C) *Prox1*$^{\Delta LIV}$ livers [yellow arrows point to C/EBPα$^+$/Hnf4α$^-$ cells (B) or C/EBPα$^+$/Hnf4α$^+$ cells located outside the epithelial aggregates (C); arrowheads point to the basal membrane]. (D-I) Two classes of parenchymal structures populate the *Prox1*$^{\Delta LIV}$ liver at E15.5-E18.5: aggregates (D,E) containing a mixture of cholangiocytes (Sox9$^+$/Hnf4α$^-$, yellow arrowheads), hepatocytes (Hnf4α$^+$/Sox9$^-$, white arrows), and hybrid cells (Hnf4α$^+$/Sox9$^+$, yellow arrows) and ductal structures (F-I) with prominent lumens (asterisks in F) and a basal membrane (arrowheads) expressing mostly cholangiocyte markers [e.g. Sox9 (arrow in F, arrowhead in G)], apical osteopontin (arrows in G-I), claudin7 (yellow arrows in H,I). The yellow arrow in F indicates an Hnf4α$^+$/Sox9$^+$ cell in a hybrid aggregate. Scale bars: 25 μm (B-F,H); 50 μm (A,G,I).

phenotypic alteration, because *Lamb1* expression increases in fetal liver explants treated with TGFβ.

We observed that some epithelial aggregates in the parenchyma of *Prox1*$^{\Delta LIV}$ livers contained a mixture of cholangiocytes (i.e. Sox9$^+$/Hnf4a$^-$ cells), hepatocytes (i.e. Hnf4a$^+$/Sox9$^-$ cells) and hybrid cells (i.e. Hnf4a$^+$/Sox9$^+$ cells). Parenchymal aggregates expressing cholangiocyte and hepatocyte markers were also reported in the livers of mouse embryos lacking *Cebpa*, *Hnf6*, *Oc-2* or *Hhex* (Hunter et al., 2007; Clotman et al., 2005; Yamasaki et al., 2006). However, almost all cells in the epithelial aggregates of *Prox1*$^{\Delta LIV}$ livers expressed Hnf6, and similarly, the parenchymal aggregates of *Hnf6/Oc-2* double knockout livers expressed Prox1 broadly (supplementary material Fig. S7). These paradoxical results underscore the complexity of interactions among the different transcription factors controlling the fate of hepatic cells. By contrast, the expression of C/EBPα rapidly decayed in *Prox1*$^{\Delta LIV}$ livers after E12.5, becoming almost negligible in numerous parenchymal aggregates at E15.5 (supplementary material Fig. S3C). These results argue that Prox1 activity may be necessary to maintain the expression of C/EBPα in hepatocyte precursors.

One major difference between *Prox1*$^{\Delta LIV}$ embryos and embryos lacking *Cebpa*, *Hnf6*, *Oc-2* or *Hhex* (Hunter et al., 2007; Clotman et al., 2005; Yamasaki et al., 2006) is that parenchymal structures displaying features of bona fide bile ducts (i.e. expressed cholangiocyte markers but not hepatocyte markers, had apicobasal polarity, and had lumens) developed only in the liver of *Prox1*$^{\Delta LIV}$ embryos. Interestingly, these ectopic biliary structures were especially abundant towards the hilar region and in the vicinity of portal veins, which indicates that specific local cues probably played a role in their formation. We hypothesize that the periportal TGFβ gradient proposed by Clotman et al. (Clotman et al., 2005) contributed to the formation of ectopic bile ducts in *Prox1*$^{\Delta LIV}$ livers, because this signaling pathway is a known inducer of biliary development (Lemaigre, 2009; Si-Tayeb et al., 2010). Therefore, the presence of both hybrid cholangiocyte-hepatocyte aggregates and

Development (2014) doi:10.1242/dev.099481

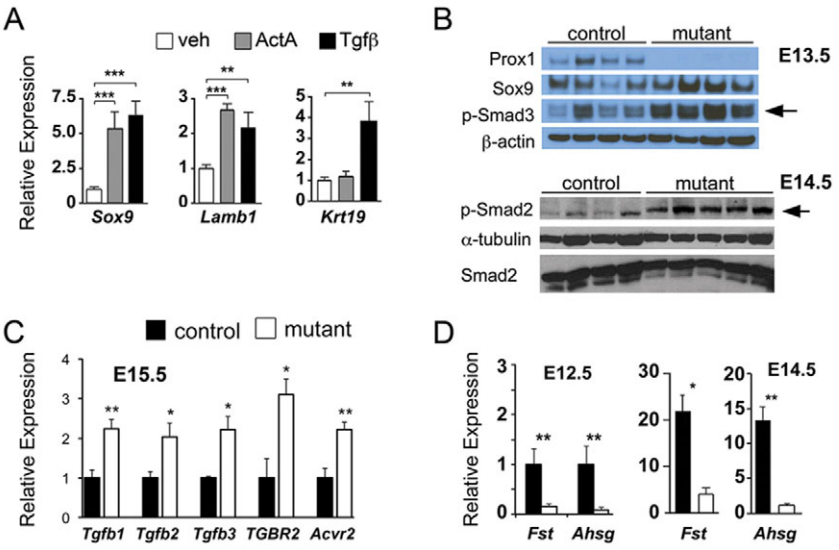

Fig. 7. TGFβ signaling is increased in *Prox1*-depleted livers. (A) E12.5 wild-type liver explants maintained in culture for 24 hours with 200 ng/ml recombinant TGFβ or activin A (ActA) express more *Sox9* or *Lamb1* transcripts than do vehicle-treated (veh) explants. TGFβ treatment also increases *Krt19* expression in fetal liver explants (data represent the mean ± s.e.m. of three to five independent experiments). (B) Western blot results show increased levels of phospho-Smad3 (E13.5) and phospho-Smad2 (E14.5) proteins in extracts of individual mutant livers compared with control livers (notice that Sox9 expression also increases in *Prox1*-deficient extracts). (C) qRT-PCR results show increased expression of transcripts encoding TGFβ ligands (*Tgfb1/2/3*) and TGFβ/activin receptors (*Tgbr2*, *Acvr2*) in E15.5 $Prox1^{\Delta LIV}$ livers. (D) qRT-PCR results show reduced expression of the TGFβ/activin signaling inhibitors *Fst* and *Ahsg* in $Prox1^{\Delta LIV}$ livers compared with control livers at E12.5 and E14.5 (*n*=3-4 specimens per genotype). Data represent the mean ± s.e.m. of three to five independent experiments. **P*<0.05, ***P*<0.01, ****P*<0.001.

bona fide biliary structures in the parenchyma of *Prox1*-deficient liver may indicate that although cholangiocyte specification is the default fate of hepatic precursors, full activation of a biliary program requires specific inductive cues. In conclusion, our study demonstrates that Prox1 activity is necessary to specify the hepatocyte cell fate of liver precursors.

Premature, abnormal intrahepatic bile duct morphogenesis occurs upon Prox1 inactivation

$Prox1^{\Delta LIV}$ livers have an excess of cells expressing Sox9 around the portal vein branches as early as E12.5. Two major results in our study supported that this alteration was a consequence of enhanced cholangiocyte cell commitment: (1) *Prox1* ablation did not increase the proliferation of ductal plate cells or PDS and (2) deleting *Prox1* in hepatic cells after E13.5 (i.e. most likely after cholangiocyte cell fate has been specified) did not result in biliary hyperplasia. However, it is unclear why bile ducts formed prematurely in $Prox1^{\Delta LIV}$ livers.

Intrahepatic bile duct morphogenesis is a sequential process involving the formation of a single layer of $Sox9^{+}$/$Hnf4\alpha^{-}$ cholangiocytes (ductal plate), asymmetric periportal structures expressing Sox9 on the portal side and Hnf4α on the parenchymal side (PDSs), and symmetric tubular structures ($Sox9^{+}$) displaying apicobasal polarity and lumens (bile ducts) (Antoniou et al., 2009). Interestingly, we found that tubular morphogenesis did not follow the same pattern in *Prox1*-depleted livers. Specifically, clusters of $Sox9^{+}$ cells but not single-layered ductal plates were noticed in the periportal areas of the mutant liver at E12.5. These cellular aggregates contained a mixture of cells expressing Sox9, Hnf4α or both and were surrounded by a basal membrane. By E15.5, when most biliary structures in wild-type liver consist of ductal plates and PDSs (Antoniou et al., 2009), nearly all cholangiocytes in the periportal areas of the *Prox1*-depleted liver formed large tubular structures resembling more mature bile ducts. The presence of a basal membrane probably helped advance the biliary morphogenetic program, including lumen formation and acquisition of apicobasal polarity in the early periportal epithelial aggregates lacking *Prox1* function, because hepatic progenitors maintained in culture in laminin-111-containing gel give rise to ductal structures lined by polarized biliary cells (Tanimizu et al., 2007). Moreover, a recent study (Tanimizu et al., 2012) showed that bile duct morphogenesis requires signals mediated by α1- and α5-containing laminins.

It is possible that newly committed cholangiocytes of $Prox1^{\Delta LIV}$ livers respond better to local TGFβ signals because they lack inhibitors of this pathway. Hence, increased TGFβ responsiveness in combination with other signaling pathways (e.g. Notch) could have triggered biliary morphogenesis prematurely in $Prox1^{\Delta LIV}$ livers. In turn, enhanced bile duct formation probably lead to excessive deposition of extracellular matrix proteins and expansion of mesenchymal cells, because in injured livers the formation of ductular structures is accompanied by deposition of collagens and expansion of fibroblastic cells (Desmet et al., 1995). Finally, increased production of TGFβ ligands probably contributed to those alterations because this cytokine is a known inducer of fibrosis in the adult liver (Bataller and Brenner, 2005).

In summary, $Prox1^{\Delta LIV}$ mice represent a novel animal model of intrahepatic bile duct malformation resulting from excessive commitment of biliary precursor cells (Raynaud et al., 2011; Strazzabosco and Fabris, 2012).

Prox1 is a novel regulator of the hepatocyte phenotype

Loss of Prox1 function severely affected the expression of numerous hepatocyte metabolic genes, altered hepatocyte morphogenesis and disrupted hepatocyte architecture. The death of $Prox1^{\Delta LIV}$ mice immediately after birth further supported the hypothesis that Prox1 activity is essential for proper hepatocyte development.

One major finding of our study is that parenchymal hepatoblasts require Prox1 to initiate proper hepatocyte gene expression. Lack of Prox1 activity could alter hepatocyte transcription directly, as suggested by a recent study (Charest-Marcotte et al., 2010) showing that Prox1 binds the promoter region of various hepatocyte genes in adult livers. Interestingly, some of the proposed Prox1 hepatocyte target genes (*Apoc3*, *Ces3*, *Cyp3a11*, *ApoH*, *Apoc2* and *Klf15*) showed reduced expression in $Prox1^{\Delta LIV}$ livers as early as E12.5.

Although in general hepatocyte transcripts were largely decreased in $Prox1^{\Delta LIV}$ livers, we identified a handful of hepatocyte metabolic transcripts (e.g. *Apoa4*, *Cyp7a1* and *Ldhb*) that were upregulated when Prox1 function is absent. Two of those transcripts (*Cyp7a1* and *Ldhb*) are known targets of hepatic nuclear receptors (NRs): *Cyp7a1* was a target of Nr5a2 and Hnf4α, whereas *Ldhb* is a potential target of ERRα. Interestingly, protein-protein interactions

Development (2014) doi:10.1242/dev.099481

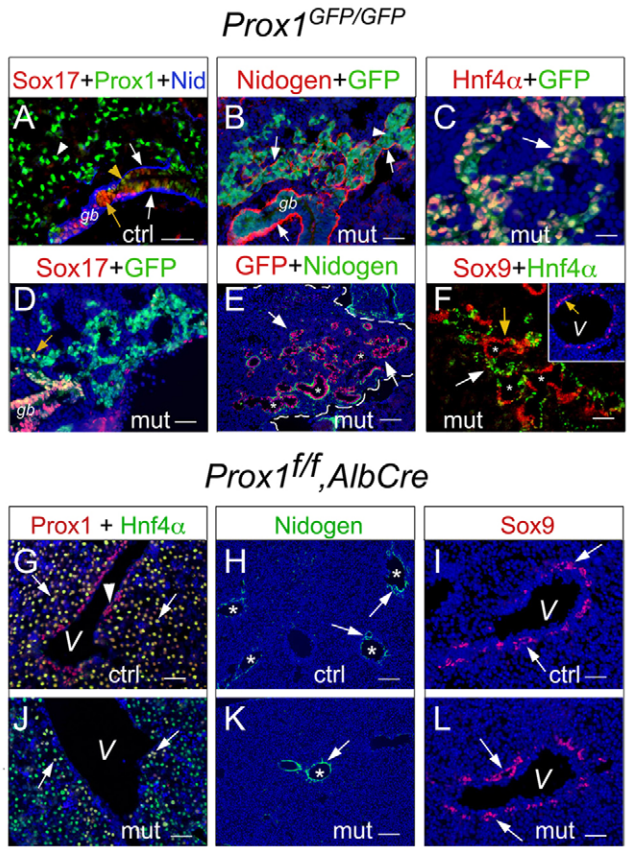

Fig. 8. *Prox1*-nullizygous livers, but not livers with *Prox1* ablation in committed hepatic cells, have increased cholangiocyte formation. (A) Prox1 is highly expressed in hepatoblasts (white arrowhead) and poorly expressed (yellow arrowhead) in the gall bladder (gb) epithelium ($Sox17^+$) in E11.5 wild-type embryos (arrows indicate the basal membrane surrounding the gall bladder). Yellow arrow indicates Sox17 expression in the gall bladder. (B) Hepatoblasts (GFP^+, arrowhead) form an epithelium contiguous to the gall bladder in E11.5 *Prox1*-nullizygous ($Prox1^{GFP/GFP}$) embryos. Arrows indicate the basal membrane surrounding the mutant hepatic epithelium. (C,D) The E11.5 $Prox1^{GFP/GFP}$ hepatic epithelium expresses Hnf4α (arrow in C) but not Sox17 (yellow arrow in D) indicates a single pair of $Sox17^+$ cells located close to the gall bladder). (E) The E14.5 $Prox1^{GFP/GFP}$ hepatic epithelium (GFP^+) is covered with a $nidogen^+$ basal membrane (arrows), displays prominent lumens (asterisks), and is confined to the hilar region (the broken line demarcates the liver periphery). (F) Numerous cells express Sox9 (yellow arrow), and fewer cells express Hnf4α (white arrow) in the E14.5 $Prox1^{GFP/GFP}$ hepatic epithelium. At this stage, only a few $Sox9^+$ cells are seen around the portal vein in E14.5 wild-type livers (inset). (G) Prox1 is expressed in both hepatocytes (arrows, $Hnf4α^+$) and cholangiocytes (arrowhead, $Hnf4α^-$) of E18.5 wild-type livers. (J) Very few hepatocytes express Prox1 in E18.5 $Prox1^{f/f}$;*AlbCre* livers. (H,I,K,L) E18.5 wild-type (H,I) and $Prox1^{f/f}$;*AlbCre* (K,L) livers have similar expression of nidogen (H,K) and Sox9 (I,L) around periportal areas. Arrows indicate expression of nidogen (H,K) or Sox9 (I,L) restricted to periportal areas. *V* and asterisks indicate portal veins. Cell nuclei were stained with DAPI in B-E and G-L. Scale bars: 25 µm (C), 50 µm (A,B,D,F,G,I,J,L); 100 µm (E,H,K).

between Prox1 and each of those NRs have been described in HepG2 cells or adult liver extracts (Charest-Marcotte et al., 2010; Qin et al., 2004; Song et al., 2006), with Prox1 acting as a transcriptional co-repressor in the resulting complex. This negative effect of Prox1 on NR function could explain why the expression of *Cyp7a1* and *Ldhb* increased following *Prox1* ablation. Of note, defective regulation of Nr5a2 and Hnf4α activities could have a broader impact in hepatocyte transcription, because these NRs are important core components of the hepatic transcription factor network (Kyrmizi et al., 2006).

In summary, we demonstrated that Prox1 is a novel, crucial regulator of cell differentiation and morphogenesis during hepatogenesis. In addition, we found that Prox1 activity is necessary to establish metabolic transcription correctly in hepatocyte precursors. Therefore, we propose that Prox1 is a novel component of the hepatocyte transcriptional regulatory network. Our findings bear significance to improving *in vitro* programming of stem cell differentiation to hepatocytes for cellular therapy of liver disease.

MATERIALS AND METHODS

Mice

$Prox1^{floxP/+}$ mice and $Prox1^{GFP\text{-}Cre/+}$ mice (G. Oliver, St Jude Children's Research Hospital, Memphis, TN, USA), *Foxa3cre* mice (K. H. Kaestner, University of Pennsylvania, Philadelphia, PA, USA) and *AlbCre* mice (*B6.Cg-Tg[Alb-cre]21Mgn/J*, Jackson Laboratories, Bar Harbor, ME, USA) were maintained and genotyped as described previously (Harvey et al., 2005; Lee et al., 2005; Postic et al., 1999; Srinivasan et al., 2010). $Rosa26^{EYFP}$ mice (Srinivas et al., 2001) were also obtained from the Jackson Laboratory. *HNF6/OC2* double-knockout mice were obtained as previously described (Clotman et al., 2005). Mice were treated according to the criteria outlined in the Guide for the Care and Use of Laboratory Animals of the National Institutes of Health. All experiments were reviewed and approved by the St Jude Animal Care and Use Committee and by the Ethical Committee of the Université Catholique de Louvain.

Processing of embryos and liver tissues

Tissues of dissected embryos or livers of newborn mice were prepared for immunohistochemical or *in situ* hybridization analyses as previously described (Wang et al., 2005). Paraffin-embedded tissues were processed for immunohistochemical or histological analyses as described by Westmoreland et al. (Westmoreland et al., 2009).

Immunohistochemical analysis

For immunohistochemical analysis, tissue sections were incubated in primary antibody overnight at room temperature. Supplementary material Table S1 provides a full list of the antibodies used and the experimental conditions. Images were obtained with a Zeiss Axioskop 2 microscope. Images were processed using Adobe Photoshop version 7.0 (Adobe Systems).

In situ hybridization analysis

In situ hybridization was performed on sections, as described by Wang et al. (Wang et al., 2004). The *Ahsg* probe was obtained by RT-PCR using total RNA isolated from the E14.5 mouse liver and the following primers: 5′-GCTGCCTTCAACACACAGAA-3′ (forward) and 5′-ATGTCCTGTCT-GCCAAAACC-3′ (reverse) to amplify a 500-bp fragment. The plasmid used to prepare the *Tgfb1* RNA probe was kindly provided by H. L. Moses (Vanderbilt University, Nashville, TN, USA).

Quantitative real-time PCR

RNAs were isolated using TRIzol (Invitrogen) or an RNeasy Micro Kit for E12.5 livers (Qiagen), and cDNA was prepared using the SuperScript First-Strand Synthesis System for RT-PCR (Invitrogen). Quantitative real-time PCR (qRT-PCR) was performed on a Mastercycler realplex machine (Eppendorf). Expression levels were determined with gene-specific primers (supplementary material Table S5) and SYBR Green reagent. *Gapdh* expression was used to normalize gene expression levels.

Microarray analysis

Gene expression analyses were performed at the Hartwell Center for Bioinformatics and Biotechnology at St. Jude Children's Research Hospital. The Affymetrix Mouse Genome 430 2.0 GeneChip array (Affymetrix) was used. Total RNA was prepared using TRIzol. An Agilent 2100 Bioanalyzer was used to confirm RNA quality (Agilent Technologies). Total RNA

samples (5-10 µg) were processed according to the Affymetrix Gene Expression Technical Manual (2006; http://media.affymetrix.com/support/downloads/manuals/expression_analysis_technical_manual.pdf). Expression signals were calculated by the MAS5 statistical algorithm and the Affymetrix GCOS software (version 1.4), and detection calls were determined using the GeneChip Operating software (GCOS; Affymetrix). Expression profiles in mutant and wild-type samples were compared using the pair-wise method in GCOS. Microarray data have been deposited in Gene Expression Omnibus under accession number GSE36583.

Western blot analysis

Liver samples from mouse embryos were homogenized in RIPA buffer containing protease inhibitors and phosphatase inhibitors. Antibodies recognizing phospho-Smad3 or phospho-Smad2 proteins used for western blotting are listed in supplementary material Table S1.

Liver explant experiments

E12.5 livers were dissected into four parts that were maintained separately in culture on Millicell-CM culture plate inserts (Millipore) as previously described (Clotman et al., 2005), with or without recombinant TGFβ or activin A (200 ng/ml of either agent) (R&D Systems). Explants were maintained in culture for 24 hours.

Chromatin immunoprecipitation (ChIP) in HepG2 cells

HepG2 cells were treated for 15 minutes with 3% paraformaldehyde in PBS, washed in PBS, and collected. Whole-cell extracts were sonicated five times for 10 seconds each at 15-µm amplitude (Sanyo Soniprep 150), pre-cleared using normal rabbit serum and salmon sperm DNA, and incubated with specific antibodies (supplementary material Table S1) overnight at 4°C. After washing the immunoprecipitates, we eluted the DNA-antibody complexes; the crosslinking was reversed, and DNA was purified by QIAquick kit (Qiagen). Quantitative real-time PCR analysis was performed using 2 µl ChIP sample per 25 µl reaction, and normalized to input DNA. The qPCR primers were verified using tenfold serially diluted DNA. Primers used to amplify the Prox1-binding element in the *Fst* promoter were 5′-TGTCACTGAACAGGTGTGGT-3′ and 3′ TCACCATGACTCTTGC-CATC-5′.

Isolation of Dlk1^{+} fetal liver cells

Dlk1^{+} hepatoblasts were isolated from E12.5 wild-type mouse livers via fluorescence-activated cell sorting (FACS) per published methods (Tanimizu et al., 2003). The primary antibody was anti-Dlk1/Pref-1 (MBL #D187-3), and the secondary antibody was phycoerythrin-conjugated anti-rat IgG. RNA from FACS-sorted Dlk1^{+} cells and Dlk1^{-} cells was extracted using the Qiagen RNeasy Micro Kit.

Statistical analyses

All experiments were performed at least thrice. Values are expressed as mean ± s.e.m. Results were analyzed using unpaired Student's *t*-test. Differences with $P<0.05$ were considered statistically significant.

Acknowledgements

We thank G. Oliver for providing the *Prox1*$^{loxP/+}$ and *Prox1*$^{GFP\text{-}Cre/+}$ mouse strains; L. Paul for help isolating fetal liver RNA; the Hartwell Center, the FACS Core Facility, and the Cell and Tissue Imaging Core of St. Jude; N. Shiojiri and S. Hupert for technical advice; and A. McArthur for editing the manuscript.

Competing interests

The authors declare no competing financial interests.

Author contributions

B.S.-P. conceived the study and wrote the manuscript. A.S. and J.Y. performed the majority of experiments. N.Y. and F.G. assisted with the western blotting, qRT-PCR and liver-explant experiments. D.C.B. performed the ChIP assays. G.A.N. assisted with the microarray data analyses. P.K.B. provided expertise and reagents for the ChIP assays. S.C. and F.P.L. analyzed Prox1 expression in *Onecut1/Onecut2* livers. K.H.K. provided mice and expertise. All authors contributed to the manuscript's final version.

Funding

This work was funded by the National Institute of Diabetes and Digestive and Kidney Diseases [ARRA5R01DK080069 to B.S.-P.]; the American Lebanese Syrian Associated Charities (ALSAC); the D. G. Higher Education and Scientific Research of the French Community of Belgium [ARC 10/15-029 to F.P.L.]; the Fund for Scientific Medical Research (Belgium); and the Interuniversity Attraction Poles (IAP) Program (Belgian Science Policy). Deposited in PMC for release after 12 months.

Supplementary material

Supplementary material available online at
http://dev.biologists.org/lookup/suppl/doi:10.1242/dev.099481/-/DC1

References

Antoniou, A., Raynaud, P., Cordi, S., Zong, Y., Tronche, F., Stanger, B. Z., Jacquemin, P., Pierreux, C. E., Clotman, F. and Lemaigre, F. P. (2009). Intrahepatic bile ducts develop according to a new mode of tubulogenesis regulated by the transcription factor SOX9. *Gastroenterology* **136**, 2325-2333.

Bataller, R. and Brenner, D. A. (2005). Liver fibrosis. *J. Clin. Invest.* **115**, 209-218.

Burke, Z. and Oliver, G. (2002). Prox1 is an early specific marker for the developing liver and pancreas in the mammalian foregut endoderm. *Mech. Dev.* **118**, 147-155.

Carey, G. B. and Chang, N. S. (1998). Cloning and characterization of a transforming growth factor beta 1-induced anti-apoptotic adhesion protein TIF2. *Biochem. Biophys. Res. Commun.* **249**, 283-286.

Charest-Marcotte, A., Dufour, C. R., Wilson, B. J., Tremblay, A. M., Eichner, L. J., Arlow, D. H., Mootha, V. K. and Giguère, V. (2010). The homeobox protein Prox1 is a negative modulator of ERRalpha/PGC-1alpha bioenergetic functions. *Genes Dev.* **24**, 537-542.

Chen, Q., Dowhan, D. H., Liang, D., Moore, D. D. and Overbeek, P. A. (2002). CREB-binding protein/p300 co-activation of crystallin gene expression. *J. Biol. Chem.* **277**, 24081-24089.

Choksi, S. P., Southall, T. D., Bossing, T., Edoff, K., de Wit, E., Fischer, B. E., van Steensel, B., Micklem, G. and Brand, A. H. (2006). Prospero acts as a binary switch between self-renewal and differentiation in Drosophila neural stem cells. *Dev. Cell* **11**, 775-789.

Clotman, F., Jacquemin, P., Plumb-Rudewiez, N., Pierreux, C. E., Van der Smissen, P., Dietz, H. C., Courtoy, P. J., Rousseau, G. G. and Lemaigre, F. P. (2005). Control of liver cell fate decision by a gradient of TGF beta signaling modulated by Onecut transcription factors. *Genes Dev.* **19**, 1849-1854.

Cui, W., Tomarev, S. I., Piatigorsky, J., Chepelinsky, A. B. and Duncan, M. K. (2004). Mafs, Prox1, and Pax6 can regulate chicken betaB1-crystallin gene expression. *J. Biol. Chem.* **279**, 11088-11095.

Dennler, S., André, J., Verrecchia, F. and Mauviel, A. (2009). Cloning of the human GLI2 Promoter: transcriptional activation by transforming growth factor-beta via SMAD3/beta-catenin cooperation. *J. Biol. Chem.* **284**, 31523-31531.

Desmet, V., Roskams, T. and Van Eyken, P. (1995). Ductular reaction in the liver. *Pathol. Res. Pract.* **191**, 513-524.

Dudas, J., Papoutsi, M., Hecht, M., Elmaouhoub, A., Saile, B., Christ, B., Tomarev, S. I., von Kaisenberg, C. S., Schweigerer, L., Ramadori, G. et al. (2004). The homeobox transcription factor Prox1 is highly conserved in embryonic hepatoblasts and in adult and transformed hepatocytes, but is absent from bile duct epithelium. *Anat. Embryol. (Berl.)* **208**, 359-366.

Harvey, N. L., Srinivasan, R. S., Dillard, M. E., Johnson, N. C., Witte, M. H., Boyd, K., Sleeman, M. W. and Oliver, G. (2005). Lymphatic vascular defects promoted by Prox1 haploinsufficiency cause adult-onset obesity. *Nat. Genet.* **37**, 1072-1081.

Hassan, B., Li, L., Bremer, K. A., Chang, W., Pinsonneault, J. and Vaessin, H. (1997). Prospero is a panneural transcription factor that modulates homeodomain protein activity. *Proc. Natl. Acad. Sci. USA* **94**, 10991-10996.

Hunter, M. P., Wilson, C. M., Jiang, X., Cong, R., Vasavada, H., Kaestner, K. H. and Bogue, C. W. (2007). The homeobox gene Hhex is essential for proper hepatoblast differentiation and bile duct morphogenesis. *Dev. Biol.* **308**, 355-367.

Kyrmizi, I., Hatzis, P., Katrakili, N., Tronche, F., Gonzalez, F. J. and Talianidis, I. (2006). Plasticity and expanding complexity of the hepatic transcription factor network during liver development. *Genes Dev.* **20**, 2293-2305.

Lavado, A., Lagutin, O. V., Chow, L. M., Baker, S. J. and Oliver, G. (2010). Prox1 is required for granule cell maturation and intermediate progenitor maintenance during brain neurogenesis. *PLoS Biol.* **8**, e1000460.

Lee, C. S., Friedman, J. R., Fulmer, J. T. and Kaestner, K. H. (2005). The initiation of liver development is dependent on Foxa transcription factors. *Nature* **435**, 944-947.

Lemaigre, F. P. (2009). Mechanisms of liver development: concepts for understanding liver disorders and design of novel therapies. *Gastroenterology* **137**, 62-79.

Lozier, J., McCright, B. and Gridley, T. (2008). Notch signaling regulates bile duct morphogenesis in mice. *PLoS ONE* **3**, e1851.

Lüdtke, T. H., Christoffels, V. M., Petry, M. and Kispert, A. (2009). Tbx3 promotes liver bud expansion during mouse development by suppression of cholangiocyte differentiation. *Hepatology* **49**, 969-978.

Nakamura, T., Takio, K., Eto, Y., Shibai, H., Titani, K. and Sugino, H. (1990). Activin-binding protein from rat ovary is follistatin. *Science* **247**, 836-838.

Postic, C., Shiota, M., Niswender, K. D., Jetton, T. L., Chen, Y., Moates, J. M., Shelton, K. D., Lindner, J., Cherrington, A. D. and Magnuson, M. A. (1999). Dual roles for glucokinase in glucose homeostasis as determined by liver and pancreatic beta cell-specific gene knock-outs using Cre recombinase. *J. Biol. Chem.* **274**, 305-315.

Qin, J., Gao, D. M., Jiang, Q. F., Zhou, Q., Kong, Y. Y., Wang, Y. and Xie, Y. H. (2004). Prospero-related homeobox (Prox1) is a corepressor of human liver receptor homolog-1 and suppresses the transcription of the cholesterol 7-alpha-hydroxylase gene. *Mol. Endocrinol.* **18**, 2424-2439.

Raynaud, P., Tate, J., Callens, C., Cordi, S., Vandersmissen, P., Carpentier, R., Sempoux, C., Devuyst, O., Pierreux, C. E., Courtoy, P. et al. (2011). A classification of ductal plate malformations based on distinct pathogenic mechanisms of biliary dysmorphogenesis. *Hepatology* **53**, 1959-1966.

Shiojiri, N. and Sugiyama, Y. (2004). Immunolocalization of extracellular matrix components and integrins during mouse liver development. *Hepatology* **40**, 346-355.

Si-Tayeb, K., Lemaigre, F. P. and Duncan, S. A. (2010). Organogenesis and development of the liver. *Dev. Cell* **18**, 175-189.

Song, K. H., Li, T. and Chiang, J. Y. (2006). A Prospero-related homeodomain protein is a novel co-regulator of hepatocyte nuclear factor 4alpha that regulates the cholesterol 7alpha-hydroxylase gene. *J. Biol. Chem.* **281**, 10081-10088.

Sosa-Pineda, B., Wigle, J. T. and Oliver, G. (2000). Hepatocyte migration during liver development requires Prox1. *Nat. Genet.* **25**, 254-255.

Spence, J. R., Lange, A. W., Lin, S. C., Kaestner, K. H., Lowy, A. M., Kim, I., Whitsett, J. A. and Wells, J. M. (2009). Sox17 regulates organ lineage segregation of ventral foregut progenitor cells. *Dev. Cell* **17**, 62-74.

Srinivas, S., Watanabe, T., Lin, C. S., William, C. M., Tanabe, Y., Jessell, T. M. and Costantini, F. (2001). Cre reporter strains produced by targeted insertion of EYFP and ECFP into the ROSA26 locus. *BMC Dev. Biol.* **1**, 4.

Srinivasan, R. S., Geng, X., Yang, Y., Wang, Y., Mukatira, S., Studer, M., Porto, M. P., Lagutin, O. and Oliver, G. (2010). The nuclear hormone receptor Coup-TFII is required for the initiation and early maintenance of Prox1 expression in lymphatic endothelial cells. *Genes Dev.* **24**, 696-707.

Strazzabosco, M. and Fabris, L. (2012). Development of the bile ducts: essentials for the clinical hepatologist. *J. Hepatol.* **56**, 1159-1170.

Suzuki, A., Sekiya, S., Büscher, D., Izpisúa Belmonte, J. C. and Taniguchi, H. (2008). Tbx3 controls the fate of hepatic progenitor cells in liver development by suppressing p19ARF expression. *Development* **135**, 1589-1595.

Szweras, M., Liu, D., Partridge, E. A., Pawling, J., Sukhu, B., Clokie, C., Jahnen-Dechent, W., Tenenbaum, H. C., Swallow, C. J., Grynpas, M. D. et al. (2002). alpha 2-HS glycoprotein/fetuin, a transforming growth factor-beta/bone morphogenetic protein antagonist, regulates postnatal bone growth and remodeling. *J. Biol. Chem.* **277**, 19991-19997.

Tanimizu, N. and Miyajima, A. (2004). Notch signaling controls hepatoblast differentiation by altering the expression of liver-enriched transcription factors. *J. Cell Sci.* **117**, 3165-3174.

Tanimizu, N., Nishikawa, M., Saito, H., Tsujimura, T. and Miyajima, A. (2003). Isolation of hepatoblasts based on the expression of Dlk/Pref-1. *J. Cell Sci.* **116**, 1775-1786.

Tanimizu, N., Miyajima, A. and Mostov, K. E. (2007). Liver progenitor cells develop cholangiocyte-type epithelial polarity in three-dimensional culture. *Mol. Biol. Cell* **18**, 1472-1479.

Tanimizu, N., Kikkawa, Y., Mitaka, T. and Miyajima, A. (2012). α1- and α5-containing laminins regulate the development of bile ducts via β1 integrin signals. *J. Biol. Chem.* **287**, 28586-28597.

Tchorz, J. S., Kinter, J., Müller, M., Tornillo, L., Heim, M. H. and Bettler, B. (2009). Notch2 signaling promotes biliary epithelial cell fate specification and tubulogenesis during bile duct development in mice. *Hepatology* **50**, 871-879.

Uemura, M., Hara, K., Shitara, H., Ishii, R., Tsunekawa, N., Miura, Y., Kurohmaru, M., Taya, C., Yonekawa, H., Kanai-Azuma, M. et al. (2010). Expression and function of mouse Sox17 gene in the specification of gallbladder/bile-duct progenitors during early foregut morphogenesis. *Biochem. Biophys. Res. Commun.* **391**, 357-363.

Wang, J., Elghazi, L., Parker, S. E., Kizilocak, H., Asano, M., Sussel, L. and Sosa-Pineda, B. (2004). The concerted activities of Pax4 and Nkx2.2 are essential to initiate pancreatic beta-cell differentiation. *Dev. Biol.* **266**, 178-189.

Wang, J., Kilic, G., Aydin, M., Burke, Z., Oliver, G. and Sosa-Pineda, B. (2005). Prox1 activity controls pancreas morphogenesis and participates in the production of "secondary transition" pancreatic endocrine cells. *Dev. Biol.* **286**, 182-194.

Westmoreland, J. J., Wang, Q., Bouzaffour, M., Baker, S. J. and Sosa-Pineda, B. (2009). Pdk1 activity controls proliferation, survival, and growth of developing pancreatic cells. *Dev. Biol.* **334**, 285-298.

Westmoreland, J. J., Kilic, G., Sartain, C., Sirma, S., Blain, J., Rehg, J., Harvey, N. and Sosa-Pineda, B. (2012). Pancreas-specific deletion of Prox1 affects development and disrupts homeostasis of the exocrine pancreas. *Gastroenterology* **142**, 999-1009, e6.

Wigle, J. T. and Oliver, G. (1999). Prox1 function is required for the development of the murine lymphatic system. *Cell* **98**, 769-778.

Yamasaki, H., Sada, A., Iwata, T., Niwa, T., Tomizawa, M., Xanthopoulos, K. G., Koike, T. and Shiojiri, N. (2006). Suppression of C/EBPalpha expression in periportal hepatoblasts may stimulate biliary cell differentiation through increased Hnf6 and Hnf1b expression. *Development* **21**, 4233-4243.

Zaret, K. S. (2002). Regulatory phases of early liver development: paradigms of organogenesis. *Nat. Rev. Genet.* **3**, 499-512.

Zong, Y., Panikkar, A., Xu, J., Antoniou, A., Raynaud, P., Lemaigre, F. and Stanger, B. Z. (2009). Notch signaling controls liver development by regulating biliary differentiation. *Development* **136**, 1727-1739.

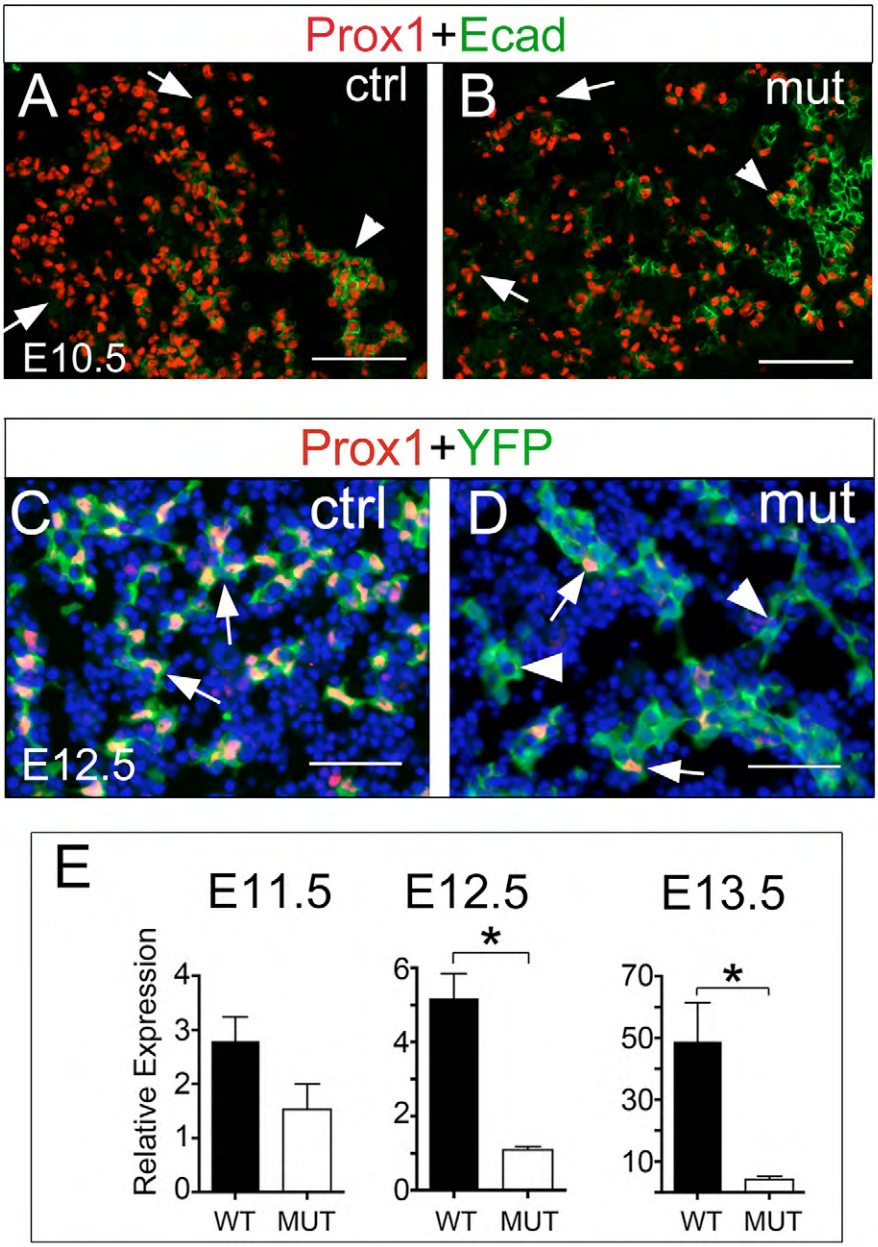

Supplementary Figure 1. *Prox1*-deletion in hepatoblasts of *Prox1*$^{\Delta LIV}$ embryos occurs post-delamination. (**A**) Prox1-expressing hepatoblasts (red, arrows) extensively colonize the liver lobes in both control (left) and *Prox1*-deficient (right) embryos dissected at E10.5 (the Ecad^{+}/Prox1^{-} area [arrowhead] in the mutant specimen is adjacent to the gut tube). (**B**) Prox1 (arrows) is expressed in all YFP^{+} cells (arrows) in E12.5 *control*^{YFP} livers (left panel), and only in very few YFP^{+} cells (arrows) in E12.5 *Prox1*$^{\Delta LIV\text{-}YFP}$ livers (left panel). (**C**) qRT-PCR results show gradual reduction of *Prox1* transcript levels in *Prox1*$^{\Delta LIV}$ livers after E11.5 (n = 3-4 specimens per genotype). **p*<0.05. Cell nuclei were stained with DAPI in **C,D**. Scale bars: 50 µm.

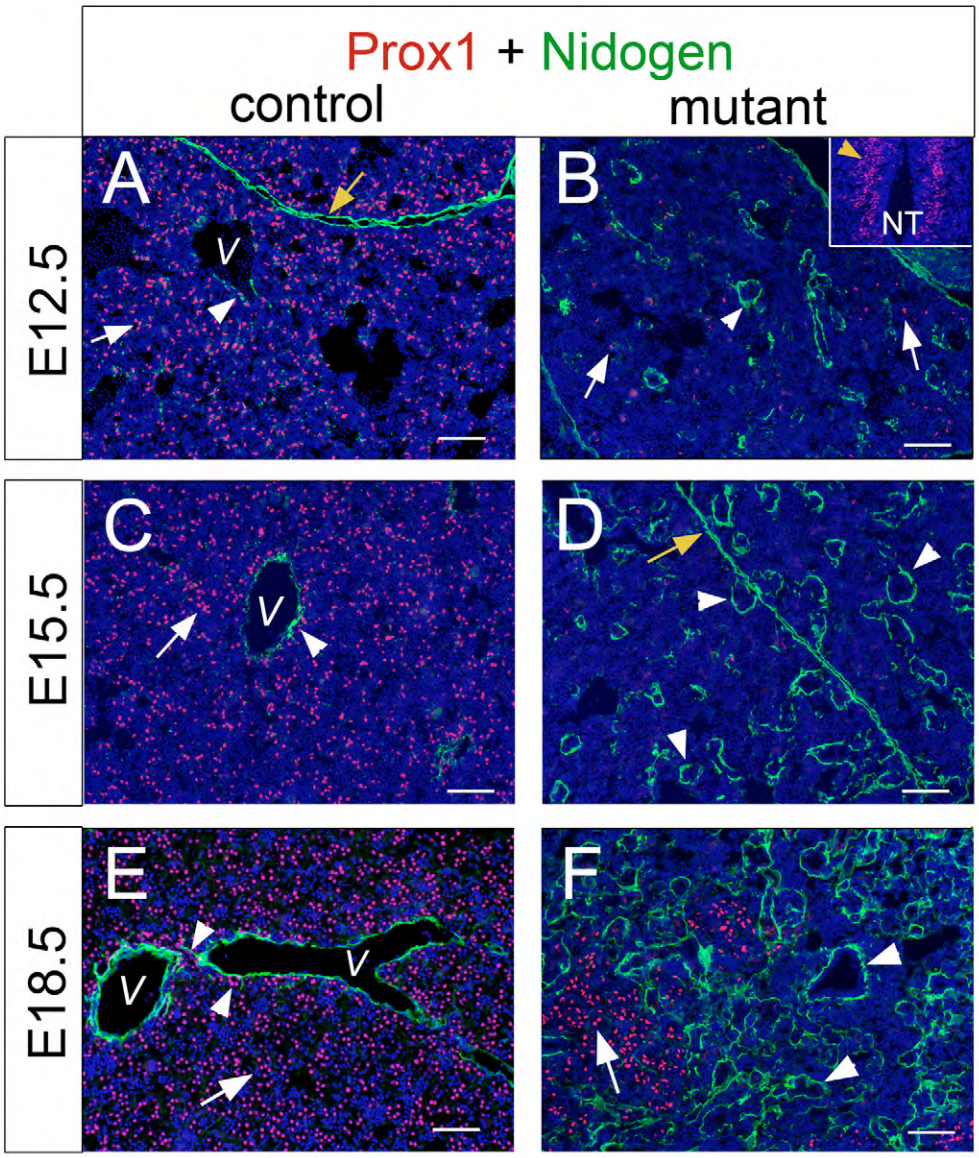

Supplementary Figure 2. Abnormal epithelial aggregates form in the liver parenchyma following *Prox1*-ablation. (**A,C,E**) Prox1 expression is observed throughout the liver parenchyma (arrows), in periportal areas (arrowheads in **A,C**), and in developing bile ducts (arrowheads in **E**), in E12.5-E18.5 control livers. (**B,D,F**) Prox1 expression is almost negligible in E12.5-E15.5 *Prox1*$^{\Delta LIV}$ livers (**B,D,** arrows), and is absent in large areas of E18.5 *Prox1*$^{\Delta LIV}$ livers (**F**). Different from control livers (**A,C,E**), numerous cellular aggregates covered with a nidogen-rich basal membrane and lacking Prox1 expression (**B,D,F**, arrowheads) are present throughout the parenchyma in E12.5-E18.5 *Prox1*$^{\Delta LIV}$ livers. Inset in **B** shows Prox1 expression [yellow arrowhead] in the neural tube [NT]). The arrow in **F** shows that hepatic cells retaining Prox1 expression do not have a basal membrane. *V*, portal vein branches; yellow arrows indicate nidogen expression at the edge of the liver lobes. Cell nuclei were stained with DAPI. Scale bars: 100 µm.

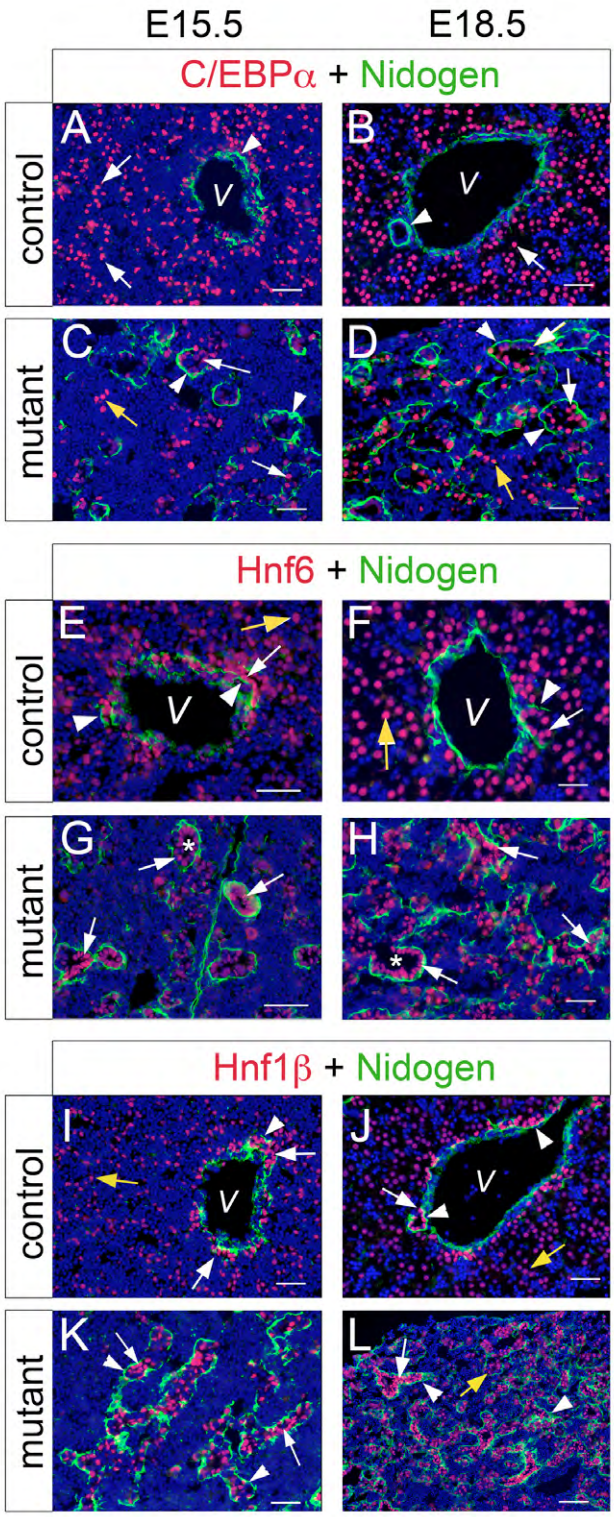

Supplementary Figure 3. Broad expression of Hnf6 and Hnf1β, and restricted expression of C/EBPα, is observed in the parenchymal aggregates of *Prox1*$^{\Delta LIV}$ livers. (**A,B**) C/EBPα is expressed throughout the liver parenchyma (arrows in **A,B**), but not in PDS (arrowhead in **A**) or bile ducts (arrowhead in **B**), in E15.5-E18.5 control livers. (**C,D**) Very few C/EBPα^{+} cells (arrows) are seen within the nidogen-rich epithelial aggregates (arrowheads) in the parenchyma of *Prox1*$^{\Delta LIV}$ livers at E15.5 (**C**) or E18.5 (**D**). (**E**) Hepatocytes express low Hnf6 (yellow arrow) and cholangiocytes (white arrow) express high Hnf6, in E15.5 control livers. (**F**) Hnf6 is highly expressed in both, bile ducts (white arrows) and hepatocytes (yellow arrow), in E18.5 control livers (arrowheads in **E,F** indicate the bile duct basal membrane). (**G,H**) Hnf6 is highly expressed in parenchymal aggregates (arrows) of E15.5 (**G**) and E18.5 (**H**) *Prox1*$^{\Delta LIV}$ livers (asterisks indicate the lumen in some ectopic biliary structures). (**I,J**) Hepatocytes express low Hnf1β (yellow arrows) and cholangiocytes (white arrows) express high Hnf1β, in E15.5-E18.5 control livers. (**K**) Hnf1β (arrows) is highly expressed in parenchymal aggregates (arrowheads) of E15.5 *Prox1*$^{\Delta LIV}$ livers. (**L**) Higher expression of Hnf1β is observed in parenchymal structures resembling bile ducts (white arrow), compared to parenchymal aggregates lacking a lumen (yellow arrow), in E18.5 *Prox1*$^{\Delta LIV}$ livers. Cell nuclei were stained with DAPI. Scale bars are 50 μm, except in **L** (100 μm).

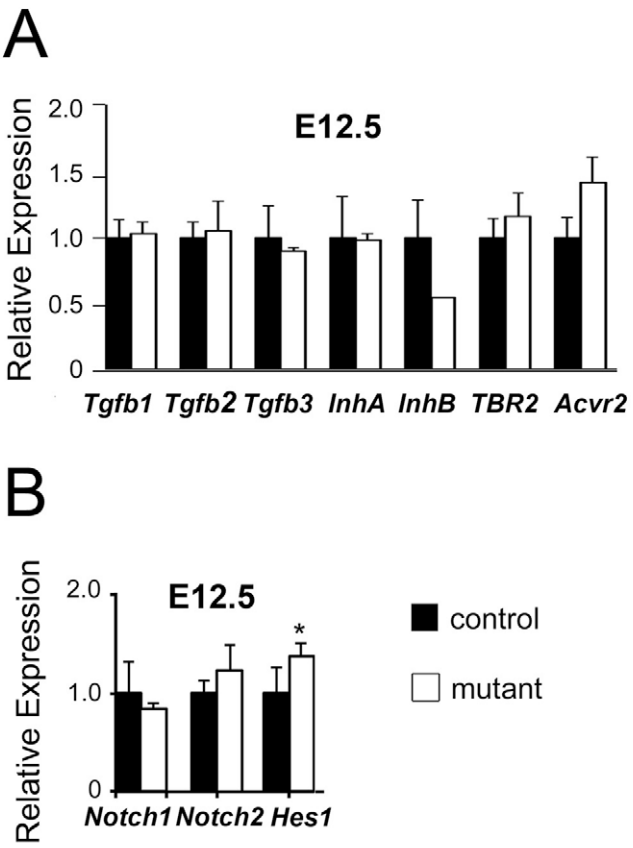

Supplementary Figure 4. Loss of *Prox1* does not affect the early hepatic expression of ligands or receptors of Notch signaling and TGFβ **signaling.** (**A**) qRT-PCR results show comparable expression of transcripts encoding *Tgfb1, Tgfb2, Tgfb3, InhibinA, InhibinB, Acvr2,* and *TGFBR2,* between control and *Prox1*$^{\Delta LIV}$ livers dissected at E12.5. (**B**) qRT-PCR results also show comparable expression levels of transcripts encoding the Notch1 and Notch2 receptors, and a very mild increment in the expression of transcripts encoding the Notch effector Hes-1, in E12.5 *Prox1*$^{\Delta LIV}$ livers (n= 3-4 specimens per genotype; *p<0.05).

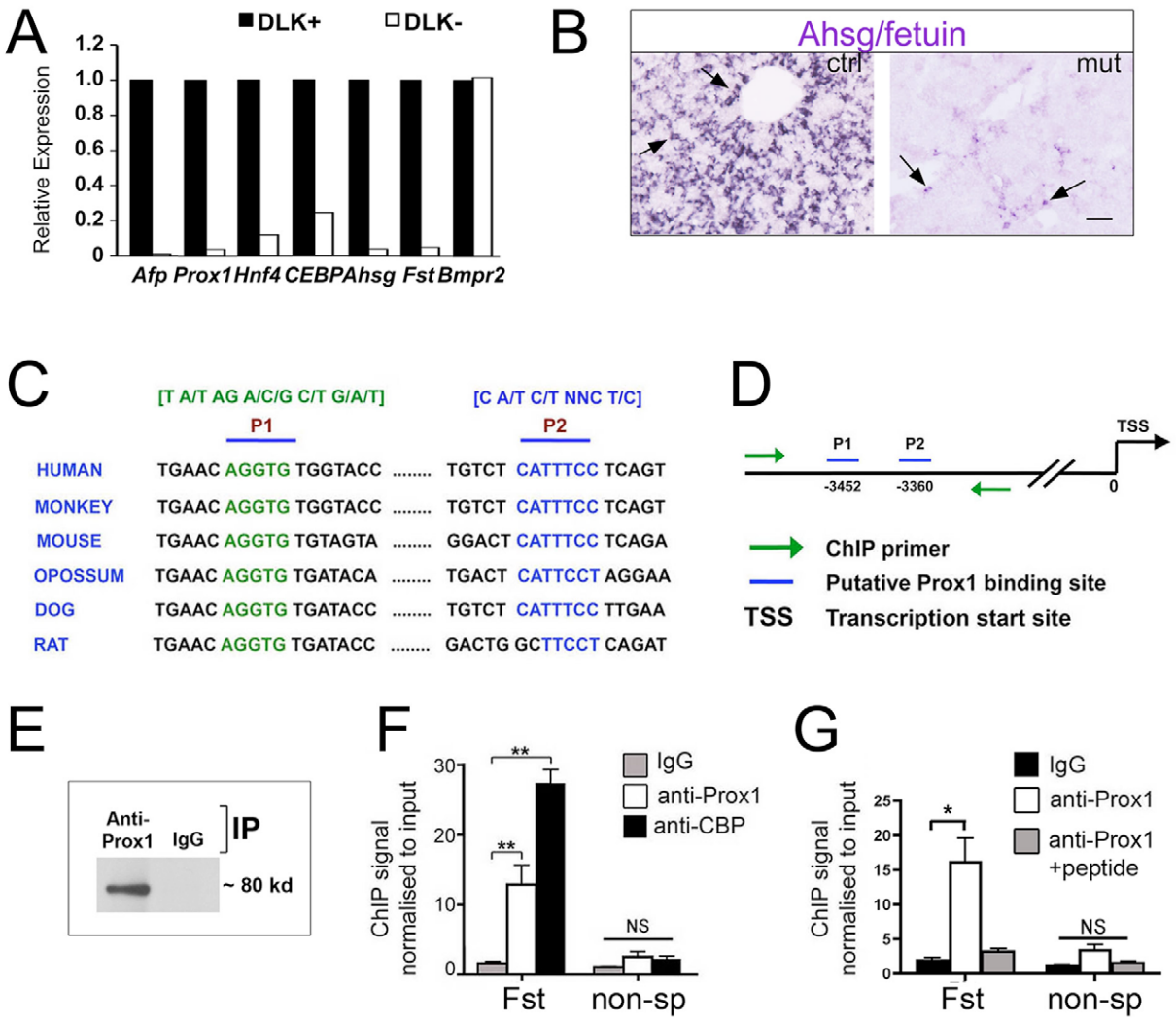

Supplementary Figure 5. *Fst* is a novel Prox1 target gene in hepatoblasts. A) qRT-PCR results show enriched expression of the hepatoblast transcripts *Afp*, *Prox1*, *Hnf4a*, *Cebpa,* and expression of *Ahsg* and *Fst*, in Dlk^{+} cells purified by FACS (results are from ten pooled E12.5 wild-type livers). (**B**) In situ hybridization results show abundant *Ahsg* expression in parenchymal cells of control livers (left), and almost no *Ahsg* expression in *Prox1*$^{\Delta LIV}$ livers (right) at E13.5 (scale bar is 50 µm). (**C**) DNA sequences of the *Fst* regulatory region from various vertebrate genes were compared to identify evolutionary conserved regions of DNA (www.ecrbrowser.dcode.org) and analyzed for putative Prox1 or prospero (the *Drosophila* structural homologue of Prox1) binding motifs (Choksi et al., 2006; Cui et al., 2004; Hassan et al., 1997). Two potential Prox1-binding motifs were identified at approximately 3.3Kb (**P2**) and 3.4Kb (**P1**) upstream of the *Fst* transcriptional start site. (**D**) Schematic view of the *Fst* gene showing the location of putative Prox1 binding sites and the primer pair used to detect enrichment of this regulatory element by using ChIP. (**E**) The Prox1 antibody used for ChIP assay was able to bind and precipitate Prox1 in whole cell lysates from HepG2 cells. (**F**) ChIP results from HepG2 cells show significant enrichment using anti-Prox1 antibodies of the region of the *Fst* promoter containing putative Prox1-binding sites (labeled "Fst") in comparison with IP with rabbit IgG. IP with antibodies recognizing the transcriptional coactivator CREB-binding protein (CBP), which is known to interact with Prox1 (Chen et al., 2002), also enriched the same region of the *Fst* promoter in comparison with IP with rabbit IgG. There was no significant enrichment of chromatin located ~20Kb upstream of the *Fst* transcriptional start site (labeled as "non-sp" or non-specific) after IP with either anti-Prox1 or anti-CBP antibodies. (**G**) The enrichment of the putative Prox1-binding region in the *Fst* promoter of HepG2 cells chromatin by the Prox1 antibody is abolished when Prox1 peptide is added to the antibody (the Prox1 C-terminal peptide sequence VPEIFKSPNCLQELL was synthesized and used to block the activity of the antibody). Data represent the mean (±SEM) of 3-5 independent experiments. *p<0.05, **p<0.01, ***p<0.001, NS= not significant.

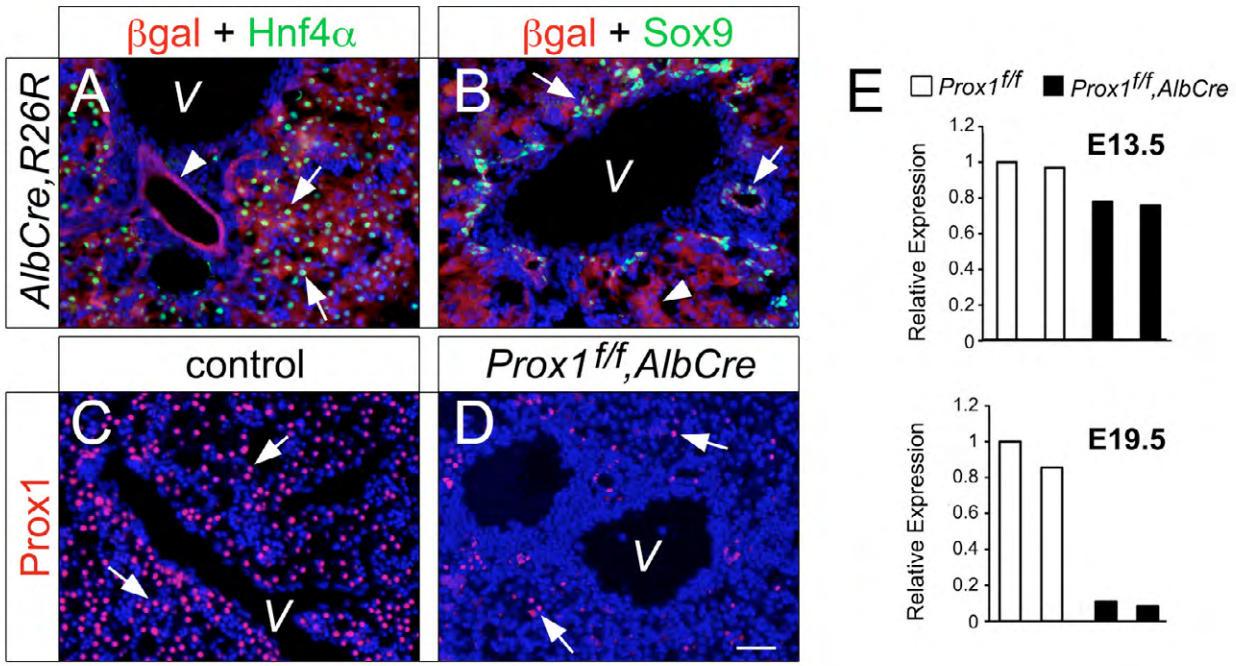

Supplementary Figure 6. *Prox1* is effectively deleted in *Prox1$^{f/f}$,AlbCre* livers at E18.5-E19.5, but not at E13.5. (**A,B**) Expression of the bgal reporter protein (red) is observed in both hepatocytes (Hnf4α^{+} cells, arrows in **A**) and cholangioctes (arrowhead in **A**; Sox9^{+} cells and arrows in **B**), in E18.5 *Prox1$^{f/f}$,ROSA26R,AlbCre* livers. (**C**) Prox1 (arrows) is broadly expressed throughout the parenchyma in E18.5 control livers. (**D**) In contrast, very few cells express Prox1 (arrows) in E18.5 *Prox1$^{f/f}$,AlbCre* livers. (**E**) qRT-PCR results show slightly decreased *Prox1* expression at E13.5, and substantially reduced *Prox1* expression at E19.5, in *Prox1$^{f/f}$,AlbCre* livers compared to control livers (two individual samples per genotype were used for each time point). (**A-D**) Cell nuclei were stained with DAPI. Scale bar: 50 μm.

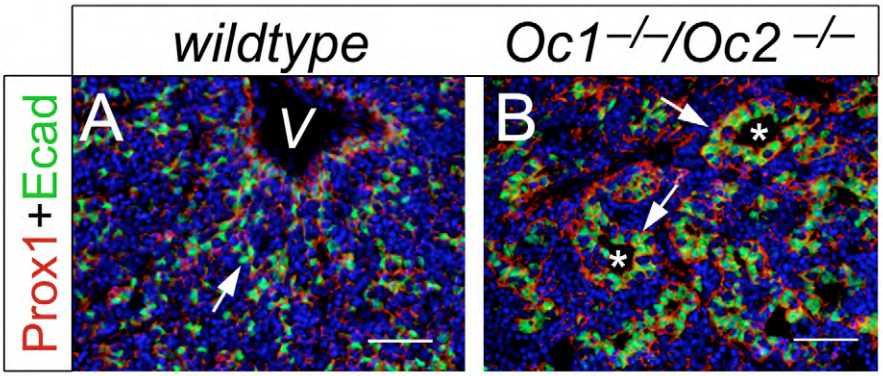

Supplementary Figure 7. Prox1 is expressed in parenchymal ductal structures in livers lacking both *Hnf6/Onecut1* and *Onecut2*. (**A**) Prox1 expression is observed in cords of parenchymal cells (arrows) in E15.5 control livers. (**B**) Prox1 expression (arrows) is also detected in tubular structures (asterisks) present in the liver parenchyma of *Hnf6/Onecu2* littermates. *V*= vein. Cell nuclei were stained with DAPI. Scale bars: 50 μm.

Supplementary Table 1. Primary Antibodies used in this study.

Antibody	Species	Company	Dilution	Application
Prox1	Rabbit	Ang-Bio	1:500	IHC (paraffin)
Prox1	Rabbit	Millipore	1:1000	IHC (frozen)
Prox1	Rabbit	Sosa-Pineda lab.	1:1000	Western Blot
E-cadherin	Rat	Sigma	1:5000	IHC (frozen)
Sox9	Rabbit	Invitrogen	1:250	IHC (WB)
Sox9	Rabbit	Millipore	1:1000	IHC (frozen/paraffin)
Sox9	Goat	Santa Cruz	1:50	IHC (frozen)
C/EBPlpha	Rabbit	Santa Cruz	1:50	IHC (frozen/paraffin)
Hnf1beta	Rabbit	ProteinTech	1:2000	IHC (frozen/paraffin)
HNF4α	Goat	Santa Cruz	1:50	IHC (frozen/paraffin)
vimentin	Guinea Pig	RDI	1:500	IHC (frozen)
GFP	Rabbit	Molecular Probe	1:1000	IHC (frozen)
GFP	Chicken	Abcam	1:1000	IHC (frozen)
Nidogen	Rat	BD Bioscience	1:5000	IHC (frozen)
Osteopontin	Goat	R&D	1:50	IHC (frozen)
Cytokeratin-19	Rat	DSHB	1:100	IHC (paraffin)
Claudin-7	Rabbit	Spring Biosc.	1:250	IHC (frozen/paraffin)
Laminin	Rabbit	Sigma	1:1000	IHC (frozen)
Collagen-IV	Rabbit	Biodesign	1:2000	IHC (frozen)
fibronectin	Rabbit	Sigma	1:2000	IHC (frozen)
PH3	Mouse	Upstate	1:2000	IHC (frozen)
CPS1	Rabbit	Abcam	1:500	IHC (frozen/paraffin)
ZO-1	Rat	Millipore	1:250	IHC (frozen)
Beta-catenin	Rabbit	Abcam	1:250	IHC (frozen)
PECAM	Rat	Pharmingen	1:250	IHC (frozen)
SMAD 3	Rabbit	Epitomics	1:1000	Western Blot
SMAD 2	Rabbit	Cell signaling	1:1000	Western Blot

p-SMAD 2	Rabbit	Cell signaling	1:1000	Western Blot
p-SMAD 3	Rabbit	Epitomics	1:1000	Western Blot
β-actin	Mouse	Sigma	1:5000	Western Blot
CBP	Rabbit	Santa Cruz		ChIP
Prox1	Rabbit	Invitrogen		ChIP
Dlk/Pref-1	Rat	MBL		FACS

Supplementary Table 2. Transcripts encoding basal membrane or cell adhesion proteins differentially expressed in *Prox1*-deficient livers identified by microarray analysis.

A: BASAL MEMBRANE TRANSCRIPTS

Gene Title	Gene Symbol	Fold Change
INCREASED		
procollagen, type XII, alpha 1	*Col12a1*	21.11
procollagen, type IV, alpha 6	*Col4a6*	11.31
tissue inhibitor of metalloproteinase 2	*Timp2*	10.56
laminin B1 subunit 1	*Lamb1-1*	6.96
matrix metallopeptidase 23	*Mmp23*	6.96
fibronectin type III domain containing 1	*Fndc1*	5.66
integrin beta 3	*Itgb3*	5.28
laminin, alpha 1	*Lama1*	4.00
matrix metallopeptidase 15	*Mmp15*	4.00
procollagen, type I, alpha 1	*Col1a1*	3.48
procollagen, type VI, alpha 1	*Col6a1*	3.03
procollagen, type V, alpha 2	*Col5a2*	2.83
procollagen, type VI, alpha 3	*Col6a3*	2.83
matrix metallopeptidase 2	*Mmp2*	2.64
integrin alpha 6	*Itga6*	2.46
matrix metallopeptidase 9	*Mmp9*	2.30
procollagen, type XXVII, alpha 1	*Col27a1*	2.00
DECREASED		
integrin alpha 4	*Itga4*	-3.25

B: CELL ADHESION TRANSCRIPTS

Gene Title	Gene Symbol	Fold Change
INCREASED		
claudin 6	*Cldn6*	55.72
claudin 2	*Cldn2*	24.25
claudin 18	*Cldn18*	21.11
claudin 7	*Cldn7*	17.15
neural cell adhesion molecule 1	*Ncam1*	16.00
claudin 3	*Cldn3*	12.13
hepatocyte cell adhesion molecule	*Hepacam*	6.96
cadherin 16	*Cdh16*	4.92
cadherin 11	*Cdh11*	3.48
CEA-related cell adhesion molecule 1	*Ceacam1*	3.03
DECREASED		
claudin 1	*Cldn1*	-2.46

C: HEPATIC STELLATE CELL/MESENCHYMAL TRANSCRIPTS

Gene Title	Gene Symbol	Fold Change
INCREASED		
platelet derived growth factor receptor, beta polypeptide	*Pdgfrb*	8.73
LIM homeobox protein 2	*Lhx2*	2.38

For details of the Affymetrix GeneChip mouse 430 2.0 array analysis, see Materials and Methods. Genes were selected if their corresponding expression in *Prox1*-deficient livers was changed by two-fold or more.

Supplementary Table 3. Hepatocyte and cholangiocyte transcripts differentially expressed in *Prox1*-deficient livers identified by microarray analysis.

A: HEPATOCYTE TRANSCRIPTS

Gene Title	Gene Symbol	Fold Change
INCREASED		
apolipoprotein A-IV	*Apoa4*	194.01
lactate dehydrogenase B/LDH2	*Ldhb*	12.13
aldehyde dehydrogenase family 1, subfamily A7	*Aldh1a7*	9.19
alcohol dehydrogenase 1 (class I)	*Adh1*	5.66
apolipoprotein C-III	*Apoc3*	3.73
cytochr.P450,fam.7,subfam.a, polypep.1	*Cyp7a1*	3.48
DECREASED		
CCAAT/enhancer binding protein (C/EBP), alpha	*Cebpa*	-2.0
ornithine transcarbamylase	*Otc*	-2.14
fibrinogen, alpha polypeptide	*Fga*	-2.30
coagulation factor V	*F5*	-2.30
protein disulfide isomerase associated 5	*Pdia5*	-2.30
fatty acid binding protein 1, liver	*Fabp1*	-2.30
liver-expressed antimicrobial peptide 2	*Leap2*	-2.30
3-hydroxybutyrate dehydrogenase, type 1	*Bdh1*	-2.46
phospholipase A1 member A	*Pla1a*	-2.64
apolipoprotein M	*Apom*	-2.64
metallothionein 4	*Mt4*	-2.64
ATP-binding cassette, sub.C (CFTR/MRP), member 6	*Abcc6*	-3.03
fibrinogen, B beta polypeptide	*Fgb*	-3.03
coagulation factor VII	*F7*	-3.03
kininogen 1	*Kng1*	-3.48
inter-alpha trypsin inhibitor, heavy chain 3	*Itih3*	-3.73

cystathionase (cystathionine gamma-lyase)	*Cth*	-4.92
carbamoyl-phosphate synthetase 1	*Cps1*	-4.92
acyl-Coenzyme A oxidase 2, branched chain	*Acox2*	-5.66
apolipoprotein H	*Apoh*	-5.28
apolipoprotein C-II	*Apoc2*	-5.28
cytochrome P450, family 2, subfamily c, polypeptide 44	*Cyp2c44*	-5.66
apolipoprotein F	*Apof*	-5.66
glucokinase regulatory protein	*Gckr*	-6.06
Kruppel-like factor 15	*Klf15*	-6.89
glycine decarboxylase	*Gldc*	-6.50
cytochrome P450, family 2, subfamily d, polypep. 26	*Cyp2d26*	-8.57
cytochrome P450, family 2, subfamily d, polypeptide 10	*Cyp2d10*	-9.19
alpha-2-HS-glycoprotein	*Ahsg*	-11.31
kallikrein B, plasma 1	*Klkb1*	-13.93
ceruloplasmin	*Cp*	-19.70
cytochr.P450, fam.3,subfam.a, polypep.11	*Cyp3a11*	-24.25
carboxylesterase 3	*Ces3*	-24.25

B: CHOLANGIOCYTE TRANSCRIPTS

Gene Title	Gene Symbol	Fold Change
INCREASED		
keratin 19	*Krt19*	11.31
SRY-box containing gene 9	*Sox9*	12.13

For details of the Affymetrix GeneChip mouse 430 2.0 array analysis, see Materials and Methods. Genes were selected if their corresponding expression in *Prox1*-deficient livers was changed by two-fold or more.

Supplementary Table 4. Genes associated with TGFβ signaling differentially expressed in *Prox1*-deficient livers identified by microarray analysis.

TGFβ PATHWAY TRANSCRIPTS

Gene Title	Gene Symbol	Fold Change
INCREASED		
left right determination factor 1	*Lefty1*	25.99
GLI-Kruppel family member GLI2	*Gli2*	9.85
TGF-beta1-induced anti-apoptotic factor 2	*Tiaf2*	6.06
activin receptor IIB	*Acvr2b*	6.06
transforming growth factor, beta 2	*Tgfb2*	4.00
transforming growth factor, beta induced	*Tgfbi*	2.14
DECREASED		
follistatin	*Fst*	-6.96
alpha-2-HS-glycoprotein	*Ahsg*	-11.31
bone morphogenic protein receptor, type II	*Bmpr2*	-12.13

For details of the Affymetrix GeneChip mouse 430 2.0 array analysis, see Materials and Methods. Genes were selected if their corresponding expression in *Prox1*-deficient livers was changed by two-fold or more.

Supplementary Table 5. Primers used in qRT-PCR experiments.

Gene	Forward primer	Reverse primer
Prox1	cgcagaaggactctctttgtc	gattgggtgatagcccttcat
Hnf4a	ctacggagcctcgagctgt	ccacacattgtcggctaaac
Nr2f2	cttcaagcgcagcgtgcgga	cctgcctctctgtacagcttcccg
Cebpa	aaacaacgcaacgtggaga	gcggtcattgtcactggtc
Esrra	aggtggacccttgcctttc	ggcatggcttacagcttct
Nr5a2	tcctggttactggagaacacg	ttgttgaacgcgacttctgt
Gata6	catcaccatcacccgacctac	ggccctggaagctgtggag
Hhex	cggacggtgaacgactacac	cttctccagctcgacggtc
Hnf1a	aggagtgtaatagggcggagt	gaggtccgttataggtgtcca
Onecut1	ggcaacgtgagcggtagttt	ttgctgggagttgtgaatgct
Hnf1b	cccctcaccatcagccaag	ggttctgagattgctggggatt
Tbx3	gaacctacctgttcccggaaa	agtgtctcgaaaacccttgc
Foxa2	catgggacctcacctgagtc	catcgagttcatgttggcgta
Krt19	gtcccagctcagcatgaaa	ataacgggcctccgtctct
Sox9	cagcaagactctgggcaag	tccacgaagggtctcttctc
Lamb1	ttgcgtgtgtttgtgatcct	atccagaggcacagtcatca
Cldn7	gccaagacttccggttcag	caagcatggccattgaaa
Cyp7a1	ggagcttatttcaaatgatcagg	ttggccagcactctgtaatg
Ldhb	catttcgtccttttcatatt	ggaggaacaagctcccttg
Apoc3	aggagtccgatatagctgtggt	tgctccagtagcctttcagg
Ces3	atgcgcctctaccctctgata	agcaaatctcaaggagccaag
Cyp3a11	tgaatatgaaacttgctctcactaaaa	ccttgtctgcttaatttcagaggt
Apoh	atgagacggtttacctgtcct	cagggttacaagcaaaactgatg
Apoc2	acctgtaccagaagacataccc	cctgcgtaagtgctcatgg
Klf15	acaggcgagaagcccttt	catctgagcgggaaaacct
Cps1	ttctgggctgtggtccatac	ggagacagcacaccaatcaa
GS	ctcgctctcctgacctgttc	ttcaagtgggaacttgctga
Tgfb1	tggagcaacatgtggaactc	cagcagccggttaccaag
Tgfb2	tggagttcagacactcaacaca	aagcttcgggatttatggtgt
Tgfb3	cgagtggctgttgaggaga	gctgaaaggtgtgacatgga
Tgfrb2	ggctctggtactctgggaaa	aatgggggctcgtaatcct
Acvr2b	tggctgttcggtttgagc	ggccatgtaccgtctggt
Fst	cctatgagggaaagtgtatcacaa	tggaatcccataggcatttt
Ahsg	gtcacagatccagccaaatg	tgagatttgccttgcagaag
Inha	gggagtgatccctggaaac	tcctcttcatggtattggcact
Inhb	cgagatcatcagctttgcag	ggttgccttcattagagacga
Notch1	ccgtgtaagaatgctggaacg	agcgacagatgtatgaagactca
Notch2	tgcctgtttgacaactttgagt	gtggtctgcacagtatttgtcat

Hes1	aaagcctatcatggagaagaggcg	ggaatgccgggagctatctttctt
Afp	tggatgtcaggacaatctgg	gcagctttgcttggacagt
Bmpr2	ctgattggacggggtcgatac	agcgagcaatgttgtcatgtt